xPath: Human-Al Diagnosis in Pathology with Multi-Criteria Analyses and Explanation by Hierarchically Traceable Evidence

HONGYAN GU, YUAN LIANG, and YIFAN XU, University of California, Los Angeles, USA CHRISTOPHER KAZU WILLIAMS, SHINO MAGAKI, NEGAR KHANLOU, HARRY VIN-

TERS, and ZESHENG CHEN, UCLA David Geffen School of Medicine, USA

SHUO NI, University of California, Los Angeles and University of Southern California, USA

CHUNXU YANG, University of California, Los Angeles and Peking University, USA

XINHAI ROBERT ZHANG, Rush University Medical Center, USA

YANG LI, Google Research, USA

MOHAMMAD HAERI, University of Kansas Medical Center, USA

XIANG 'ANTHONY' CHEN, University of California, Los Angeles, USA

Data-driven AI promises support for pathologists to discover sparse tumor patterns in high-resolution histological images. However, from a pathologist's point of view, existing AI suffers from three limitations: (*i*) a lack of comprehensiveness where most AI algorithms only rely on a single criterion; (*ii*) a lack of explainability where AI models tend to work as 'black boxes' with little transparency; and (*iii*) a lack of integrability where it is unclear how AI can become part of pathologists' existing workflow. Based on a formative study with pathologists, we propose two designs for a human-AI collaborative tool: (*i*) presenting joint analyses of multiple criteria at the top level while (*ii*) revealing hierarchically traceable evidence on-demand to explain each criterion. We instantiate such designs in xPath — a brain tumor grading tool where a pathologist can follow a top-down workflow to oversee AI's findings. We conducted a technical evaluation and work sessions with twelve medical professionals in pathology across three medical centers. We report quantitative and qualitative feedback, discuss recurring themes on how our participants interacted with xPath, and provide initial insights for future physician-AI collaborative tools.

CCS Concepts: • Human-centered computing \rightarrow Human computer interaction (HCI); • Applied computing \rightarrow Life and medical sciences; • Computing methodologies \rightarrow Machine learning.

Additional Key Words and Phrases: Human-AI collaboration; digital pathology; medical AI; meningioma

Authors' addresses: Hongyan Gu, ghy@ucla.edu; Yuan Liang, liangyuandg@ucla.edu; Yifan Xu, yifanxu@ucla.edu, 580 Portola Plaza, Room 1538, University of California, Los Angeles, Los Angeles, California, 90095, USA; Christopher Kazu Williams, ckwilliams@mednet.ucla.edu; Shino Magaki, smagaki@mednet.ucla.edu; Negar Khanlou, nkhanlou@mednet.ucla.edu; Harry Vinters, hvinters@mednet.ucla.edu; Zesheng Chen, zesheng.chen.med1@sssss.gouv.qc.ca, UCLA David Geffen School of Medicine, 757 Westwood Plaza, Pathology and Laboratory Medicine, Los Angeles, California, USA, 90095; Shuo Ni, shuoni@usc.edu, 580 Portola Plaza, Room 1538, University of California, Los Angeles and University of Southern California, Los Angeles, California, 90095, USA; Chunxu Yang, yangchunxu@pku.edu.cn, 580 Portola Plaza, Room 1538, University of California, Los Angeles and Peking University, California, 90095, USA; Xinhai Robert Zhang, xinhai_r_zhang@rush.edu, 1653 West Congress Parkway, Department of Pathology, Rush University Medical Center, Chicago, Illinois, 60612, USA; Yang Li, yangli@acm.org, Google Research, Mountain View, California, 94043, USA; Mohammad Haeri, mhaeri@kumc.edu, 3901 Rainbow Boulevard, University of Kansas Medical Center, Kansas City, Kansas, 66103, USA; Xiang 'Anthony' Chen, xac@ucla.edu, University of California, Los Angeles, 580 Portola Plaza, Room 6730A, Los Angeles, California, 90095, USA.

Permission to make digital or hard copies of all or part of this work for personal or classroom use is granted without fee provided that copies are not made or distributed for profit or commercial advantage and that copies bear this notice and the full citation on the first page. Copyrights for components of this work owned by others than ACM must be honored. Abstracting with credit is permitted. To copy otherwise, or republish, to post on servers or to redistribute to lists, requires prior specific permission and/or a fee. Request permissions from permissions@acm.org.

© 2021 Association for Computing Machinery.

XXXX-XXXX/2021/11-ART \$15.00

https://doi.org/10.1145/nnnnnnnnnnnnn

ACM Reference Format:

1 INTRODUCTION

One critical step for cancer diagnosis and treatment is pathologists' analysis of histological glass slides obtained from a patient's tissue sections to identify evidence of tumor patterns and determine the diagnosis (*e.g.*, benign *vs.* malignant) and grade based on medical guidelines.

Such an analysis is often challenging for pathologists, due to the sheer amount of effort it requires to identify sparse, small-scaled, non-homogeneous histological patterns of tumors in each patient's case. Further, the process suffers from subjectivity due to the intra- and inter-observer variations, *e.g.*, different interpretations of the grading guidelines and different ways of sampling and examining the slides to 'implement' a given guideline [14].

To overcome these challenges, digital pathology, enabled by advanced whole slide imaging techniques, promises to transform traditional manual optical microscopic examinations to be automated by data-driven artificial intelligence (AI) [29]. Specifically, there is a recent development of deep learning techniques to detect or grade carcinoma with digitized Whole Slide Images (WSI) [48], such as breast cancer [31, 50, 63], prostate cancer [58], lung cancer [64], uterine cervical cancer [21], and glioblastoma [8].

Although multiple AI-aided diagnostic systems have been designed preliminarily for pathologists [6, 16, 44, 53, 54], there remain barriers that prevent their adoption into a clinical setting. Studies indicate that various factors are in play, including a lack of concerns for clinicians' needs that undermine their motivation to accept AI for clinical usage, and a lack of workflow integration where the system is disruptive and time-consuming to use in practice [69]. Other research pointed out that medical users desire more transparency to overcome subjectivity and more interpretability to correct the model when the model makes mistakes [14, 66]. Building upon this prior work, we conducted a formative study with four board-certified pathologists that further summarizes three gaps of employing AI-enabled analysis of histological data:

- (1) The gap of **comprehensiveness**. Most AI models tend to focus on one specific criterion inferred from one specific type of histological data, while pathologists in practice use multiple criteria and data types, *e.g.*, Hematoxylin and Eosin (H&E) staining¹ for initial examination, and for instance, Ki-67 immunohistochemistry (IHC) staining² [1] to collect different information to come up with a differential diagnosis [25, 55];
- (2) The gap of **explainability**. Most AI models function as 'black boxes' and lack transparency in how they arrive at certain findings, including, locally, how an individual criterion is computed and, globally, how different criteria are combined to arrive at a diagnosis;
- (3) The gap of **integrability**: most AI models abstract histological analysis as a computational problem, yet it remains unclear how to integrate such models into pathologists' existing workflow and practices.

To fill in these gaps, we propose a human-AI collaborative workflow for pathologists with two key design ingredients.

 $^{^1\}mathrm{A}$ primary type of staining used for histopathology examinations.

²A more precise type of staining that utilizes the antibodies to highlight specific histological features, in this case, the histological pattern of mitosis.

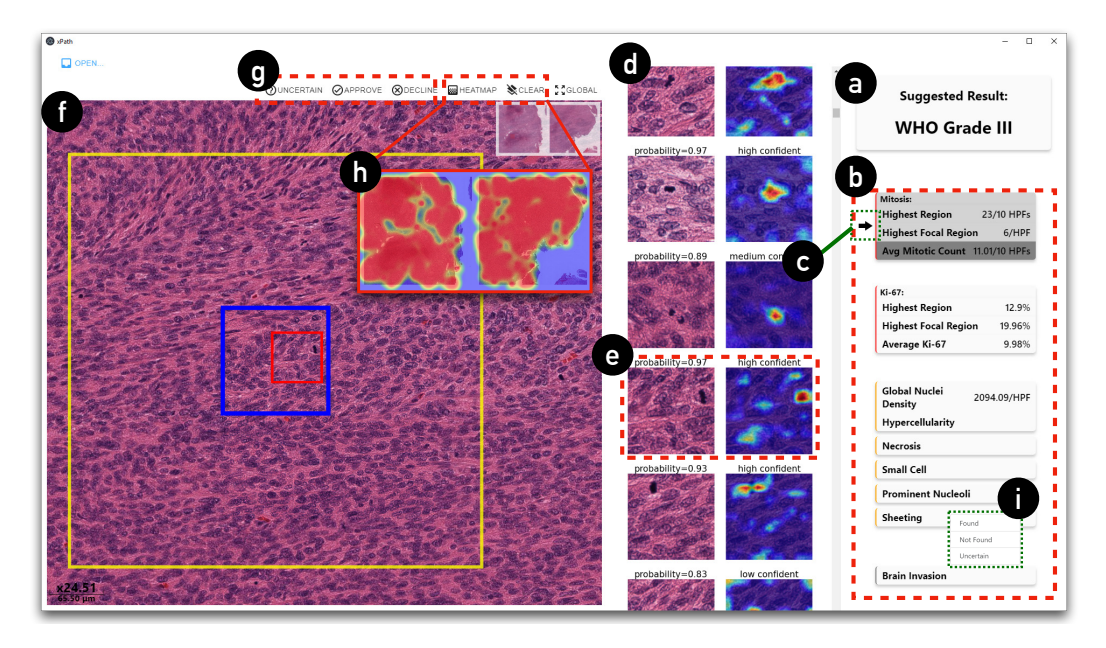


Fig. 1. A pathologist uses XPATH in a top-down workflow to oversee how multiple Al models have contributed to the grading diagnosis of meningioma — a type of brain tumor: (a) at the top-level, an Al-suggested diagnosis (*i.e.*, WHO Grade III) according to the World Health Organization guidelines, which consist of (b) a list of meningioma grading criteria examined by multiple Al models; (c) an arrow highlights the main contributing criterion to the current grading result; (d) as the user selects the histological pattern of 'mitosis' criterion, they see a list of sampled evidence based on which Al grades this criterion; (e) each piece of evidence consists of Al's output probability, confidence level, and a saliency map that highlights the spatial support for the mitosis class; (f) clicking a pair of thumbnail images registers the evidence to a whole slide image viewer with continuous magnification; the yellow outer box corresponds to the area of one high power field in the optical microscope, the blue box in the middle corresponds to a patch that includes the positive detection (a mitotic cell from xPATH's Al), while the inner red box points out a more precise location of such a detection, corresponding to the evidence in the list; (g) a user can verify each piece of sampled evidence by clicking on 'approve', 'decline' or 'declare-uncertain' button; (h) a heatmap can be enlarged to see a global distribution of each criterion; (i) the user can also override each histological feature manually. Correspondingly, the findings demonstrated in (a,b) would be updated as the user overrides or modifies the Al's results.

- Joint-analyses of multiple criteria: at the top level, we present AI's findings based on multiple juxtaposed criteria across multiple data types, which are combined to produce a single diagnosis based on rules derived from existing medical guidelines. Such a design addresses comprehensiveness by following how pathologists often examine more than one criterion; the presentation of rules addresses global explainability, i.e., how different AI-computed criteria contribute to a diagnosis.
- Explanation by hierarchically traceable evidence: for each criterion, we present a trace of evidence hierarchically across three levels: clicking a top-level finding based on a specific criterion (Figure 1b) brings a user to the mid-level list of samples (Figure 1d); The mid-level sample for the mitosis criterion consists of AI probability, confidence level and a saliency map [17] that highlights the spatial support for the mitosis class (Figure 1e); clicking one sample further brings a user to the original WSI for examining low-level details (Figure 1f). Such a design addresses local explainability by making the provenance of a criterion traceable and

transparent; further, the top-down workflow is similar to (thus integrable with) pathologists' existing practices of delegating work to trainees and overseeing their findings.

1.1 System Overview

We instantiate these two design ingredients in the implementation of xPath — a human-AI collaborative brain tumor grading tool³ for pathologists to perform top-down, multi-criterion histological analysis. In this work, the medical task of meningioma grading is selected since it represents one of the hardest practices of the pathologists — grading meningiomas is particularly challenging because it covers three aspects of difficulties for pathologists: (i) pathologists are required to locate and examine multiple histological features from cross-data-typed H&E and IHC slides, (ii) slides' high resolutions (\sim (10⁵)²) vs. small-sized histological patterns (e.g., mitosis, (\sim 90²)), and, (iii) the sparse, non-homogeneous distribution of the histological patterns. As such, the practice of grading meningiomas is a favorable arena of studying how AI should be applied to assist pathologists in carrying out the task.

Figure 1 shows an overview of xPATH 's interface. A typical workflow starts with a pathologist first seeing the top-level suggested tumor grade (Figure 1a), where an arrow (Figure 1c) highlights the main contributing criterion that leads to the suggested grading. The analysis of different criteria (Figure 1b) is produced by multiple AI models that examine histological data — H&E and Ki-67 — based on the World Health Organization (WHO) meningioma grading guideline [41]. The pathologist can further select and drill down to a specific criterion, which retrieves a set of examples as evidence (Figure 1d) to explain AI's findings. For example, for the criterion of mitotic count (the count number of a type of cell within a fixed size of area), the pathologist can see pieces of evidence (Figure 1d) detected by xPATH's mitosis classification model. Each piece of evidence (Figure 1e) demonstrates multiple explainable components, including probability, confidence level, and a saliency map. Moreover, the pathologist can open a heatmap (Figure 1h) overlaying the whole slide image to overview the density distribution of positive mitotic cells recognized by the AI. Selecting a piece of evidence directs the pathologists' attention to a high power field⁴ (HPF, yellow box) of the mitosis on the original whole slide image, where they can further examine the low-level histological features and approve/decline/declare-uncertain AI's analysis with one click (Figure 1g,i), which in turn will update AI's findings on individual criterion and, if necessary, the overall suggested grading as well based on WHO guidelines.

We conducted two evaluations to validate xPATH:

- (*i*) A technical evaluation shows AI models identifying multiple meningioma grading criteria, achieving F1 scores of 0.755, 0.904, 0.763, 0.946 in classifying four histological patterns of mitosis, necrosis, prominent nucleolus, and sheeting tissues, respectively. Moreover, models used in xPATH achieve averaged error rates of 12.08% and 29.36% in counting nuclei (for the histological pattern of hypercellularity) and calculating Ki-67 proliferation index;
- (ii) Work sessions with twelve⁵ medical professionals⁶ across three medical centers, comparing the performance of xPath with an off-the-shelf whole slide image viewer as the baseline. The result shows that, with less than an hour of learning, participants were able to use xPath to make more accurate grading decisions. Specifically, participants gave correct gradings for 7/12 cases

³Currently, we focus on the grading of meningioma—the most common primary type of brain tumor—as a point of departure for exploring the design of xPath. The goal is to aid pathologists to *grade* meningioma with the aid of AI, which assumes that tumor areas have already been identified on a slide (*e.g.*, from an early radiology examination).

⁴One high power field corresponds to a field of view under x400 magnification from the optical microscope.

⁵We would like to point out that our participants are highly-specialized medical experts that come from a much smaller population than general users and are very difficult to recruit due to their busyness.

⁶, which includes two attendings, two fellows, seven senior residents, and one junior resident.

with the baseline interface. In comparison, participants gave 17/20 cases correct gradings using xPath. In the meantime, a post-study questionnaire shows that participants found xPath more comprehensive (p=0.001), more integrable with their existing workflow (p=0.006), requiring less effort (p=0.002), and more effective on reducing the workload (p=0.002) in grading meningiomas. Moreover, they gave xPath high ratings on explainability (μ =5.58/7) and trust (μ =5.83 and 6.00/7). Last but not least, pathologists were more likely to use xPath in the future (p=0.002), and gave more overall preference on xPath (9/12 "totally prefer", 3/12 "much more prefer").

1.2 Contributions

In terms of system input, xPATH goes beyond previous work that merely relies on a single data type (e.g., H&E [24, 40, 50, 63], or immunohistochemistry examinations [3, 52, 67]); instead, xPATH's pipeline utilizes multiple H&E-based criteria (Figure 1b) and a complementary immunohistochemistry data type — Ki-67 slides as input. In terms of system output, xPATH goes beyond prior work on automating diagnosis by 'black box' AI [33, 42, 46, 70]; instead, xPATH examines whole slide images with joint analyses across multiple criteria where explanatory evidence can be traced hierarchically from top-level grading to mid-level samples and to low-level details on a whole slide image. Moreover, xPATH differs from previous medical human-AI collaboration systems [13, 19, 37] (i) by focusing on a different clinical task of diagnosing with AI, which requires an aggregation of detections and a fusion of decisions from multiple criteria and (ii) by contributing a top-down diagnosis workflow that assists pathologists in overseeing and verifying AI as a task integrable to their day-to-day work.

Our main contribution is a generalizable tool design for human-AI collaborative diagnosis that employs a workflow with joint-analyses of multiple criteria and explanation by hierarchically traceable evidence, addressing three existing gaps of comprehensiveness, explainability and integrability. Our study provides initial insights into the application of the proposed AI-assistive diagnosis, which share the common requirements of processing multiple types of medical information and overseeing AI's performance explainably from the global findings to traces of local evidence.

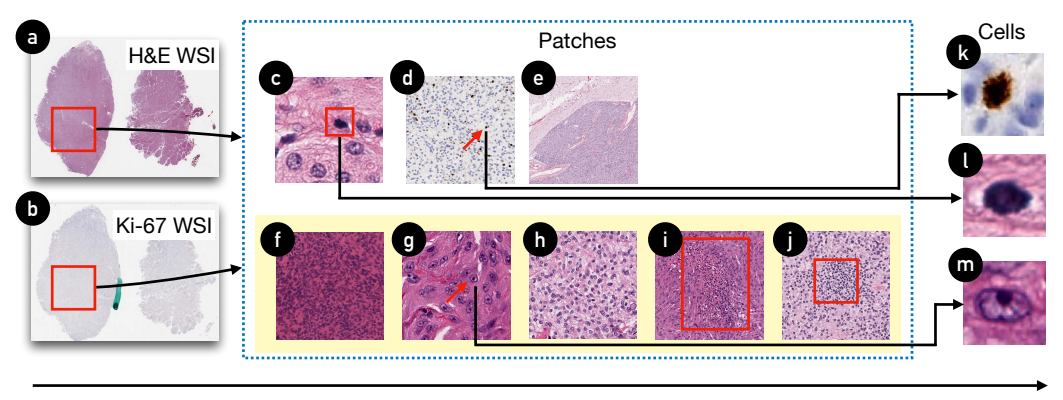
2 BACKGROUND OF MENINGIOMA

In this work, we target the challenging task of meningioma grading to probe the design of human-AI collaborative tools for pathology diagnosis.

Meningioma is the most common primary brain tumor in adults and, according to the World Health Organization (WHO) guidelines (2007), can be graded as Grade I, Grade II, or Grade III [41]. The future grading of meningioma in the new WHO guideline (2021) still recommends the same criteria for grading, although the nomenclature is slightly different.

The accurate grading of meningioma is vital for the treatment planning: the Grade I tumors can be treated with either surgery or external beam radiation, while Grade II/III ones often need both treatments [62]; meanwhile, research shows that patients with Grade III meningiomas suffer a higher recurrence rate as well as lower survival rate in comparison to Grade II patients [47].

Pathologists need to search and locate features across various magnifications in order to grade meningiomas. Specifically, they first localize the regions of interest (ROIs) in low magnification (x40), then switch to the patch level with a higher magnification (x100), and sometimes zoom further into the highest magnification (x400) into the cell level. These steps are usually repeated multiple times until pathologists have collected sufficient findings to conclude a grading and sign-off the case. Figure 2 briefly visualizes such a workflow with typical pathology slides for demonstration. Pathologists' grading workflow starts with a resected session from a patient that cuts the tumor into slices and then stains it with Hematoxylin and Eosin (H&E) solution on a glass slide (Figure 2a).



Low Magnification High Magnification

Fig. 2. An example workflow pf pathologists' grading with whole slide images (WSIs) from our formative study. (a) The resected tissues are first stained with H&E solution and scanned into WSIs. (b) An additional Ki-67 IHC staining is usually used to locate mitoses. Pathologists then zoom into the patch level and seek certain histological patterns listed in the WHO grading guidelines. Specifically, pathologists look for (c) mitotic cells (marked in the red box) in high power fields with the help of (d) Ki-67 stains; (e) brain invasion (invasive tumor cells in brain tissue); five histological patterns, including (f) hypercellularity (an abnormal excess of cells), (g) prominent nucleoli (enlarged nucleoli pointed by the arrow), (h) sheeting (loss of 'whirling' architecture), (i) necrosis (irreversible injury to cells marked in the red box), (j) small cells (tumor cell aggregation with high nuclear/cytoplasmic ratio marked in the red box). For some criteria, e.g., mitosis (k,l) and prominent nucleoli (m)), pathologists are required to zoom further into cell level for examination.

Apart from the H&E, Ki-67 immunohistochemistry (IHC) [1] is an additional staining method that is often used (Figure 2b) to provide an estimated proliferation index (Figure 2d,k), which is highly correlated to meningioma grading. Next, we describe the WHO guidelines for the meningioma grading [41]:

- **Grade I** (benign) meningiomas include "histological variant other than clear cell, chordoid, papillary, and rhabdoid "[10] *and* a lack of criteria from grade II and III meningiomas.
- **Grade II** (atypical) meningiomas are recognized by meeting at least one of the four following criteria:
 - (1) the appearance of 4 to 19 mitoses (Figure 2c,l) in 10 consecutive high-power fields (HPFs). Moreover, since mitoses are challenging to recognize in H&E, the Ki-67-positive nucleus (Figure 2k) in the corresponding areas of Ki-67 (Figure 2d) are often referred to for disambiguation;
 - (2) at least three out of five histological features are observed: hypercellularity an abnormal excess of cells in an HPF (Figure 2f), prominent nucleoli enlarged nucleoli in a cell (Figure 2g,m), sheeting loss of 'whirling' architecture (Figure 2h), necrosis irreversible injury to cells (Figure 2i), and small cell cell aggregation with high nuclear/cytoplasmic ratio (Figure 2j);
 - (3) brain invasion invasive tumor cells in brain tissue is observed (Figure 2e);
 - (4) the appearance of clear cell or chordoid histological subtype.
- **Grade III** meningiomas are justified if at least one of the following criteria met [5]:
 - (1) 20 or more mitoses per 10 consecutive HPFs;
 - (2) the appearance of frank anaplasia, papillary or rhabdoid histological subtype.

As shown above, meningioma grading is not only challenging but high-stake — an overestimated study would incur unnecessary treatment on patients, and an overlooked one would cause a delay of necessary treatment.

3 RELATED WORK

In this section, we review the related work of xPATH from three areas: (i) data-driven AI algorithms for digital pathology, (ii) tools for digital pathology, and (iii) human-AI collaborative tools.

3.1 Data-Driven AI Algorithms for Digital Pathology

According to Komura *et al.* [36], there are three primary categories of applications of data-driven AI algorithms in digital pathology: (*i*) Computer-Aided Diagnosis (CAD), (*ii*) Content-Based Image Retrieval (CBIR), and (*iii*) feature-triggered biomarker discovery. We will review the representative works on CAD, since xPATH falls into this category.

Current AI algorithms are primarily based on H&E slides, the most commonly used stained slides for providing a detailed view of the tissue. In particular, several existing approaches utilize AI algorithms to detect a single criterion in different diseases. While not targeted at meningiomas specifically, they seek the same criterion as in WHO grading guidelines [41] (e.g., mitosis). For example, Irshad et al. include selected color spaces and morphological features into the mitotic cell detection pipeline to support breast cancer grading [33]; Lu et al. use Bayesian modeling and local-region threshold method to detect mitotic cells [42]; Mishra et al. propose a CNN network to identify necrosis tissues in osteosarcoma tumor [46]; Zhou et al. enhance the traditional U-Net models by applying nested, dense skip pathways for nuclei segmentation [71]; Yap et al. use RankBoost-permutations to integrate multiple base classifiers to detect prominent nucleoli patterns from multiple tumor tissues [70].

Besides H&E slides, AI algorithms have also been devised on other stainings that can be applied in clinical settings to assist decision-making, *e.g.*, Ki-67 IHC tests. For example, Saha *et al.* use CNN as a feature extractor with Gamma Mixture Model to detect immuno-positive and negative cells in breast cancer [52]. Xing *et al.* train a fully connected convolutional network that can perform nucleus detection and classification from Ki-67 slides in a single stage [67]. Anari *et al.* utilize fuzzy c-means clustering to extract positive and negative cells for meningioma tissues [3].

Different from prior work that simply applies an AI model for predicting and red-flagging the target of a clinical task, the design of xPath has two unique features. First, previous work has been mainly based on a single staining examination as input, e.g., H&E images, which differs from clinical settings where pathologists usually refer to multiple IHC examinations to acquire comprehensive information [25, 55]. Following such practices, xPath's AI models accept multiple examinations and direct users across different input sources during diagnosis. Second, previous studies have focused on the direct prediction of the diagnostic target (e.g., classifying whether the tissue is tumor). Although some AI has reported performance on par with pathologists, the non-transparent, non-explainable characteristics of data-driven AI algorithms can still lead to distrust in high-stake medical decision processes [9]. In contrast, xPath decomposes the diagnosis as rule-based joint analyses based on multiple juxtaposed WHO criteria. By demonstrating the example-based explanations according to the criteria, xPath supports pathologists to collaborate with AI by seeing, modifying, and verifying hierarchical evidence that leads to AI's findings.

3.2 Tools for Digital Pathology

In the domain of digital pathology, multiple tools have been designed to assist pathologists for the purpose of clinical diagnosis. Rather than taking a pixel-based data-driven approach, most of these tools rely on morphological features (e.g., nuclear shape and texture). Since such features

are typically associated with attributes of the disease, they tend to have greater explainability and a stronger morphological underpinning than the ones based on data-driven models. Meanwhile, because such features are shallow and from a low level, these tools might suffer from inferior performance in diagnostic tasks and are mostly only applied for general image analysis [9]. For example, ImageJ [54], one of the most commonly used scientific image analysis tools with extensions for computational pathology, provides functions of nuclei segmentation and nuclei characteristics analysis (*e.g.*, intensity distribution and texture); Cellprofiller [16] automates morphological analysis and classifies cell phenotypes; QuPath [6] and CaMicroscope [53] provide extensive annotation and automation for nuclei segmentation and positive cell counting; Pathology Image Informatics Platform (PIIP) [44] extends Sedeen viewer⁷ by adding plugins on out-of-focus detection, region of interest transformation, and IHC slide analysis.

Despite the recent development of AI algorithms, only a few have been adapted into tools. For example, Steiner et al.'s tool can red-flag skeptical regions on slides for grading prostate biopsies and evaluate the impact of the presence of AI on inter-observer consistency and time cost [56]. Other models still lack integrability into physicians' existing workflow, which has been recognized as a long-standing issue. Teach et al. have studied physicians' attitudes on clinical consultation systems and offer suggestions on computer-based decision support systems, e.g., "minimizing changes to current clinical practices" and "enhancing the interactive capabilities" [60]. Middleton et al. have reviewed research on clinical decision support since 1990 and point out that the poor integration in clinicians' workflow is becoming a key barrier preventing the application of such tools [45]. Specifically related to histological diagnosis, there is limited research on tool design for pathologist-AI collaboration on a clinical task [13]. Different from prior work, xPATH addresses the integrability of AI using a specific task of meningioma grading as a case study. By working closely with pathologists, xPATH proposes a top-down workflow design for the tool inspired by how pathologists oversee trainees' work – presenting pathologists with a trace of evidence hierarchically from each computed criterion to contextual information and allowing pathologists to correct the AI on the fly.

3.3 Human-Al Collaborative Tools

Recent HCI research has demonstrated numerous examples of human-AI collaboration, where AI takes human input and conducts automation to ease humans' burden on performing repeated routines [18, 38, 65]. In the digital pathology domain, multiple works have shown that the human + AI team has the potential to increase the quality of diagnoses. For example, Wang *et al.* report that combining AI and human diagnoses improves pathologists' performance on breast cancer metastasis classification with an ~85% reduction of human error rate [63]. More recent work by Bulten *et al.* points out that the introduction of AI assistance increases pathologists' agreement with the expert reference standard in the prostate cancer grading [12]. Meanwhile, Buccinca *et al.* show that users might over-rely on AI by failing to recognize or correct AI when its predictions are wrong [11]. Such a contradiction in the performance opens up a question: how should human-AI collaboration be employed to harness the AI without incurring bias? To answer this question, Horvitz first sheds light on the design of human-AI collaboration by proposing a series of principles of mixed-initiative interactions [30]. Amershi *et al.* further enhance Horvitz's work with 18 design guidelines on how humans could better interact with AI, such as "support efficient correction" and "make clear why the system did what it did" [2].

However, Yang *et al.* point out that implementing these guidelines is a non-trivial task [68] — specifically, the uncertainty and complexity in AI's inference make it hard for users to control

⁷https://pathcore.com/sedeen/

the data reasoning process. Going beyond collaborative research in the general domain, Cai *et al.* highlight medical experts' need for information from AI, which includes the AI's capabilities measured in well-defined metrics and transparency to overcome subjectivity [14]. Meanwhile, merely automating a part of work would not be sufficient to motivate the medical users — a medical human-AI collaborative tool should set the explicit goal of helping medical users increase the overall quality of work [69].

A number of existing human-AI collaboration projects on pathology have been focused on Content-Based Image Retrieval (CBIR). With a given slide (or patch) from pathologists, such tools retrieve previous examples of a similar pattern to help the decision-making. For instance, Hegde *et al.* propose a reversed image searching tool to help pathologists find histological image patches of similar histological features or disease states [27]; Cai *et al.* enable pathologists to specify custom concepts that guide the retrieval of similar annotated patches of histological patterns [13]. However, CBIR focuses on image searching, which is a low-level task: what images to search, how to use the searching results, and what to conclude according to searching results. On the contrary, diagnosing/grading carcinoma in digital pathology is a high-level task, automating an aggregation of detections and a fusion of decisions from multiple criteria. This is also confirmed by Tschandl *et al.*'s work, which discovers that the CBIR tools require significantly more time to interact with than those giving diagnostic predictions [61]. In contrast to above-mentioned CBIR tools [13, 27], xPATH is considered a tool of Computer-Aided Diagnosis (CAD) or Clinical Decision Support System (CDSS).

Going beyond CBIR, existing CAD/CDSS tools enhance the detection in digital pathology with visualization. For example, Corvo et al. develop PathoVA that provides AI support for breast cancer grading by visualizing three types of pixel-level clues [19]. The system can also track pathologists' interactions and help them generate reports by providing snapshots for confirmed areas. Krueger et al. enhance users' exploration of multi-channel fluorescence images to support cell phenotype analysis [37]. Specifically, the tool maintains hierarchical statistics about the number of cell-level findings to help a user keep track of analysis and interactively update the statistics with machine learning algorithms on the fly. These tools provide a bottom-up approach to assist pathologists in making a diagnosis: pathologists are only prompted with low-level AI-generated clues (e.g., highlighting tumor cells with a segmentation map); then, the diagnosis is drawn by pathologists from fusing observations with these clues. In contrast, xPATH implements a top-down workflow, where pathologists first see an overall grading based on joint analyses of multiple criteria, then drill down to localized areas with traceable evidence and further to low-level patterns for verification and correction. Such a design provides "actionable information" [24] and reduces the total areas of study for pathologists. Moreover, to support such a workflow, xPATH makes comprehensive AI detections based on medical guidelines, whereas the above-mentioned prior studies [19, 37] only provide partial clues.

4 FORMATIVE STUDY

We conducted a formative study with four board-certified neuropathologists (average experience $\mu=21.25$ years) from a local medical center⁸ to reveal the system requirements for human-AI collaborative histological diagnosis. We started by describing the project's motivation and then asked pathologists to describe their typical process of examining a patient's case. Next, we asked them to describe the challenges in their practice and their expectations on an AI-enabled system to assist such a process.

⁸Please see the supplementary material for the demographic information for the participants.

4.1 Existing Challenges for Pathologists

We found two major challenges in the current pathology practice of meningioma grading, which validate our motivation for introducing AI into the diagnosis process.

Time consumption. The small-scaled characteristics in the patterns of interest and the very high resolution of slides make the meningioma grading highly time-consuming for pathologists. A resected section from a patient's brain tissue would generate eight to twelve H&E slides, and pathologists need to look through all those slides and integrate the information found on each slide. Except for the few experienced pathologists, meningioma grading can take up to several hours to go through a single patient's case that often consists of 10+ slides. Automating portions of the slide examination process by AI can potentially reduce such time consumption, alleviate pathologists' workload, and increase the overall throughput.

Subjectivity. There are high intra- and inter-observer variations during the grading of tumors. Pathologists summarize three factors contributing to such subjectivity: (*i*) a lack of precise definitions — the WHO guidelines do not always provide a quantified description for the five histological features for high-grade meningioma. For example, for the 'prominent nucleoli' criterion, the WHO guideline does not specify how large the nucleolus should be considered as 'prominent'; (*ii*) implementation of the examination process — for example, the mitotic count for grade II meningioma is defined as 4 to 19 mitotic cells in 10 consecutive HPFs. However, the guideline does not specify the sampling rules of these 10 HPFs. As a result, different pathologists are likely to sample different areas on the slide; (*iii*) natural variability in people, such as the level of experience, time constraint, and fatigue [20]. For AI, the definition and implementation of guidelines can be codified into the model and visualized in the system that performs consistently to overcome people's variability.

4.2 System Requirements for xPath

In addition to the two innate requirements of reducing time and overcoming subjectivity, we further identified the following requirements related to the human-AI collaborative aspects.

Comprehensiveness. The grading of tumors involves multiple sources of information (from different staining, *e.g.*, H&E, Ki-67) and criteria (*e.g.*, mitosis, nuclei density, necrosis, small cell, sheeting, prominent nucleoli, brain invasion). To incorporate хРАТН into the current practice, the system should comprehensively support all these sources and criteria.

Explainability. In lieu of a single grading result from a black-box AI model, the system should provide visual evidence to justify the AI's findings according to the medical definition of the criterion. This is because each criterion (based on histological features of an HPF) requires examining lower-level details in order to interpret an AI's finding and further needs to be traceable to the original location in the whole slide image for a review with more contextualized information. Overall, there should be explainability both globally (how results from multiple criteria are combined to yield a grading) and locally (, which includes (i) what evidence leads to the computed result of each criterion, *e.g.*, where mitoses are detected that lead to the number of mitosis counts, and (ii) why a specific piece of evidence is captured by AI, *e.g.*, which part of the evidence convinces the AI that it contains mitoses).

Integrability Similar to how attending pathologists oversee trainees' work, the system should allow pathologists to oversee AI's findings by retrieving detailed contextualized evidence ondemand. When showing the evidence of grading, the system should not overwhelm pathologists with all evidence from a whole slide; rather, it should direct pathologists to the representative regions of interest. Given that errors are inevitable for most existing AI models, the system should enable pathologists to cross-check each criterion and override the results manually when they detect an error.

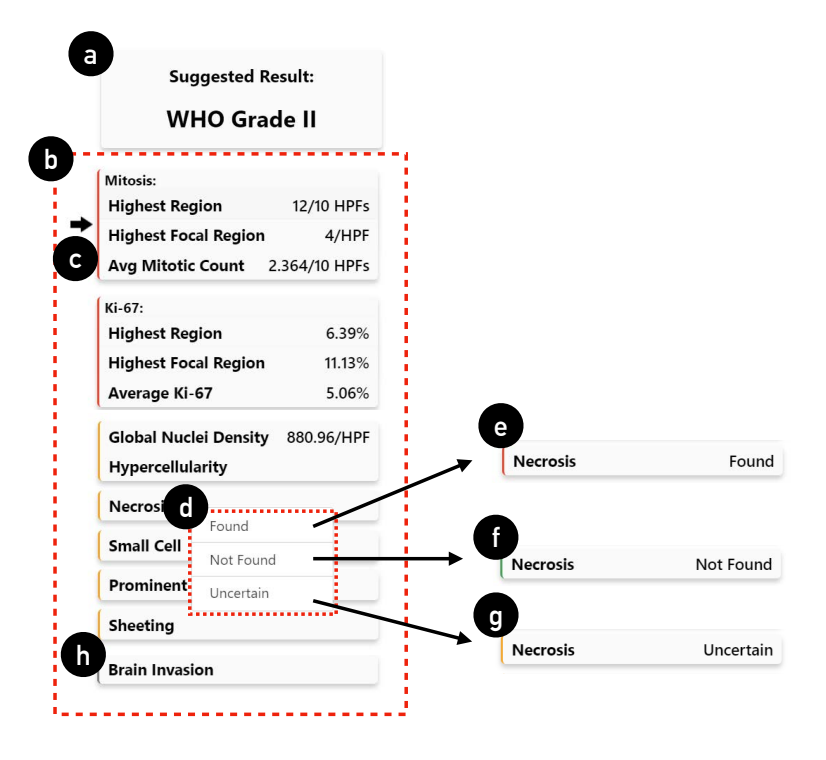


Fig. 3. Joint-analyses of multiple criteria in xPath's design: (a) the overall suggested grading; (b) a structured overview of each WHO criterion with (c) an arrow highlighting the main contributing criterion to the suggested grading; (d) users can override criteria by right-clicking on each item and change the result to 'found', 'not found' or 'uncertain'; xPath provides color bars to indicate the status of each criterion: (e) red indicates a confirmed abnormal criterion (or *presence*), (f) green indicates a confirmed normal criterion (or *absence*), (g) orange indicates the criterion is unconfirmed/confirmed uncertain, and (h) gray indicates the criterion is not applicable in this case.

5 THE DESIGN OF XPATH

Guided by the aforementioned system requirements, we developed xPATH with two key designs: (i) joint-analyses of multiple criteria and (ii) explanation by hierarchically traceable evidence. We first detail the two designs and then describe how a pathologist uses xPATH to perform a meningioma grading task.

5.1 Joint Analyses of Multiple Criteria

Based on the formative study, we found that pathologists rely on the WHO guideline to grade meningiomas, a process that involves reasoning jointly from multiple criteria. Thus xPath's design follows the WHO meningioma guideline and employs AI to compute eight criteria for meningioma grading, *i.e.*, mitotic count, Ki-67 proliferation index, hypercellularity, necrosis, small cell, prominent nucleoli, sheeting, and brain invasion⁹. Details on the AI implementation are described in Section 6. These criteria can be split into two categories: quantitative and qualitative. For the quantitative criteria of the mitotic count and Ki-67 proliferation index, we show their predicted

 $^{^{9}}$ This work does not consider using AI to identify the subtypes (e.g., clear cell, frank anaplasia) since they are easy to be discovered and justified by pathologists.

quantitative values directly. For the rest of the criteria concerned with the *presence* or *absence* of a specific histological pattern, xPATH provides recommendations of regions of interest (ROI) hotspots according to the largest aggregations of AIs' probabilities.

Figure 3 demonstrates the interface of multiple criteria. Besides showing the current suggested grading result (*i.e.*, the suggested 'WHO grade II', Figure 3a) and a structured overview of each WHO criterion (*e.g.*, mitosis, Ki-67, Figure 3b), xPATH displays an arrow to indicate the main contributing criterion that leads to the grading based on the underpinning WHO guidelines, *e.g.*, the mitotic count (Figure 3c). All the criteria are linked with ROIs related to the findings¹⁰. Moreover, AI's recommendation on all the criteria can be confirmed and modified by the pathologist. xPATH uses color bars (Figure 3e,f,g,h) to indicate the status: as shown in Figure 3, red indicates a confirmed abnormal criterion (or *presence*), green indicates a confirmed normal criterion (or *absence*), orange indicates that the criterion is unconfirmed/uncertain (neither presence nor absence), and gray indicates the criterion is not applicable in this case. Once a pathologist overrides the result of any criterion (Figure 3d), the color bar and the final grading is updated correspondingly.

In summary, the joint analysis of multiple criteria addresses comprehensiveness by following how pathologists often examine more than one criterion; the presentation of rules addresses global explainability, *i.e.*, how different AI-computed criteria are combined to arrive at a diagnosis.

5.2 Explanation by Hierarchically Traceable Evidence for Each Criterion

Another finding from the formative study is that, besides a global explanation of the overall grading, pathologists also would like to see evidence that justifies AI's grading, e.g., how AI processes the image of a local patch (for local explainability). Hence, we designed xPATH to provide such explanations by top-down, hierarchically traceable evidence. Further, such a workflow mimics a scenario that we found in the formative study: pathologists reviewing/overseeing trainees' work. By replacing trainees with AI's findings, we emulated the relationship between the pathologists and trainees to pathologist-AI collaboration, thus making AI more integral to pathologists' current practices.

As shown in Figure 4, xPATH presents a hierarchical trace of evidence for each criterion with positive findings, which allows a pathologist to see a list of mid-level samples (Figure 4c) that lead to a computed criterion (Figure 4b). For the most important criterion — mitosis, xPATH demonstrates a series of explanations in each mid-level sample, including AI's output probability (Figure 5a), AI's confidence level (Figure 5b), and a saliency map (Figure 5c) that highlights the spatial support for the mitosis class in the reference image¹¹, allowing pathologists to check AI's validity on each sample quickly. Further, at the low-level, xPATH supports registering each sample of the mid-level evidence into the whole slide image (WSI) to enable pathologists to examine in even higher magnification and search nearby for more contextual information (Figure 4d,e). With the provided mid- and low-level information, a pathologist can approve/decline/declare-uncertain a sample for a criterion with one click (Figure 4f), or return to the top-level and directly override AI's results on each criterion (Figure 4g). Correspondingly, the overall suggested grading (Figure 4a) is updated dynamically upon the user's input.

Figure 6 demonstrates typical examples of evidence provided by xPATH during the "in-the-wild" test, where we applied trained models directly on multiple H&E and Ki-67 IHC slides. Particularly, for the mitosis-related criteria (*i.e.*, mitotic count and Ki-67 proliferation index) — the most reliable

¹⁰Sampling rules of ROIs vary from different criteria. Please refer to Section 5.2 and the supplementary material for details.
¹¹Please refer to the supplementary material for the implementation of calculating the confidence level and the saliency map.

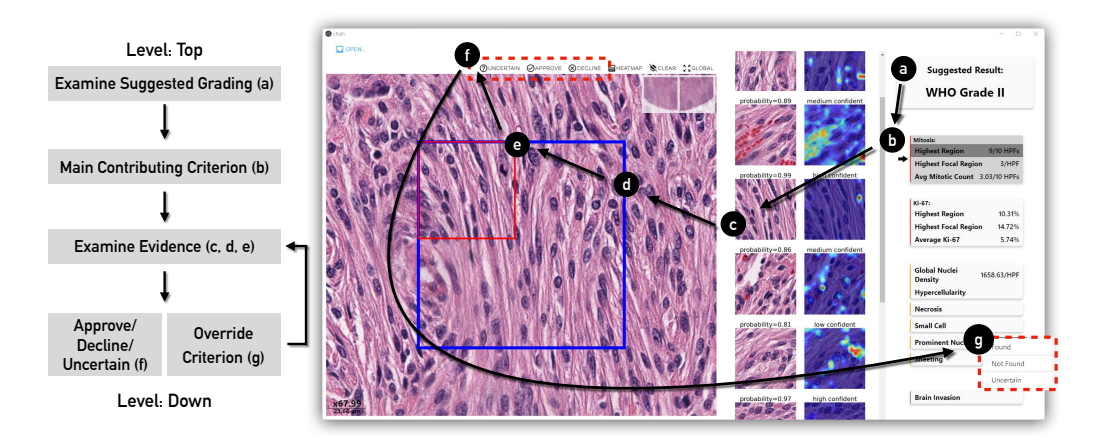


Fig. 4. We designed a top-down human-Al collaboration workflow for pathologists to interact with xPath (left) and pathologists' corresponding footprints on the xPath's frontend user interface (right). A pathologist user starts from (a) the automatically-generated suggested grading result and then examines (b) the main contributing criterion. They can further examine (c) the evidence list, and register back into the original whole slide image in higher magnifications (d,e). Furthermore, users can (f) approve/decline/declare-uncertain on the evidence, or (g) override Al results directly by right-clicking on each criterion. For the rest of the criteria, the user could repeat (c-g) until they have collected sufficient confidence for a grading diagnosis.

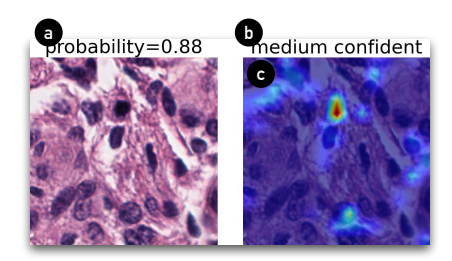


Fig. 5. For the most important criterion, mitosis, xPATH demonstrates a series of explanations in each midlevel sample, including the (a) Al's probability, (b) Al's confidence level, which is justified by the probability thresholds, and (c) a saliency map (calculated by the Grad-CAM++ algorithm [17]) that highlights the spatial support for the mitosis class in the reference image on the left.

and commonly used criteria in the grading — we introduce the two 'shortcuts' for pathologists to look into AI's results:

- **Highest Region Sampling**. One WHO criterion is "mitotic count in 10 consecutive HPFs". Our formative study found that the inter-observer consistency of "10 consecutive HPFs" is low. To address this problem, xPATH provides the highest region sampling tool. The highest region is defined as a 2 × 5 HPF area with the highest number of mitotic counts (Figure 6c) or the highest Ki-67 proliferation index (Figure 6d). This tool speeds up a pathologist's work by helping them locate 10 consecutive HPFs from the WHO guidelines.
- Highest Focal Region Sampling. From our formative study, pathologists mentioned that the high-grade meningiomas share a common feature of increased mitotic activities in a localized area. Hence, xPATH provides the highest focal sampling tool to help pathologists better localize highly concentrated mitosis/Ki-67 proliferation index areas. In xPATH, the

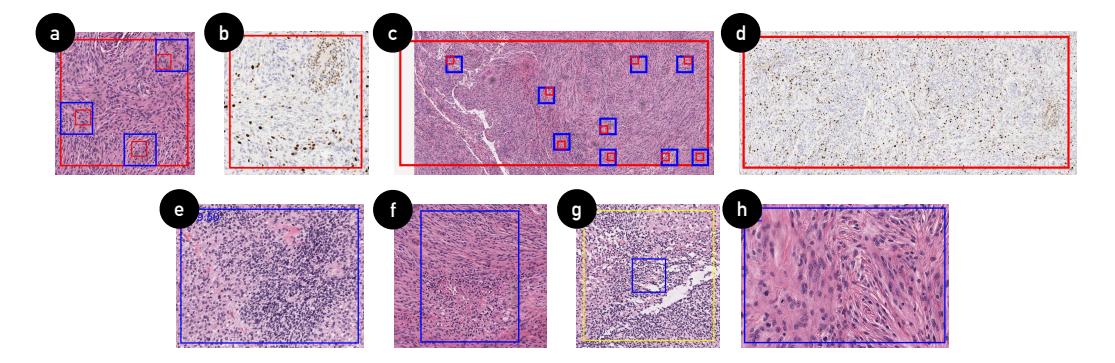


Fig. 6. Selected pieces of sampled evidence from in-the-wild detection where we applied trained models directly on multiple H&E and Ki-67 IHC slides: (a) a highest focal region sampling result of mitotic count on H&E slide (red box, 1HPF), the small blue frames are the mid-level samples (that are shown on the evidence list), the smaller red boxes in the blue frames mark the positions of mitoses found by xPATH's Al; (b) a highest focal region sampling result on the Ki-67 IHC slide (red box, 1HPF); (c) a highest region sampling result of mitotic count on H&E slide (red box, 10HPFs), the small blue frames are the mid-level samples; (d) highest region sampling result on the Ki-67 IHC slide (red box, 10HPFs); (e) a hypercellularity ROI sample (blue box); (f) a necrosis ROI sample (blue box); (g) a small cell ROI sample (the inner blue box, the outer yellow box marks the dimension of 1HPF); (h) a prominent nucleoli ROI sample (blue box).

highest focal region is calculated as the one HPF with the highest number of mitotic counts (Figure 6a) or the highest Ki-67 proliferation index (Figure 6b). Using this tool, pathologists can locate foci of highly-mitotic areas that the highest region sampling might miss.

Pathologists can go beyond the sampled areas and navigate the high-heat areas using heatmaps generated for the whole slide (please see the supplementary material for details). For example, the mitosis heatmap registers all AI-detected positive mitotic cells as a mitotic density atlas, where high-heat areas indicate a high density of mitotic cells. As such, the heatmap would serve as a 'screening tool' to help pathologists filter out unrelated areas and rapidly narrow down to the ROIs that are scattered in an entire WSI. xPATH provides such 'screening tools' for all criteria.

In summary, in contrast to prior work that enables pathologists to define their own criteria for finding similar examples [13], xPATH aims at making examination based on an existing criterion traceable and transparent with evidence, allowing pathologists to view comprehensive AI findings from multiple criteria; further, the top-down workflow is integrable with pathologists' existing practices of delegating work to trainees, which enables pathologists to oversee AI's performance.

6 IMPLEMENTATION OF XPATH'S AI BACKEND

xPath implements an AI-aided pathology image processing backend to compute the eight WHO criteria of the mitotic count, Ki-67 proliferation index, hypercellularity, necrosis, small cell, prominent nucleoli, sheeting, and brain invasion. In this section, we describe the tasks, problem formulations, datasets, and training details for the AI models. Finally, we report the performance for each of the AI models from a technical evaluation.

6.1 Tasks & Problem Formulations

In contrast to performing an image search by user-defined concepts [13], xPATH aims to screen the entire WSI to select regions of interest (ROIs) and then determine grades based on such ROIs. To achieve this, xPATH includes six AI models and two detection rules, one for each criterion, to

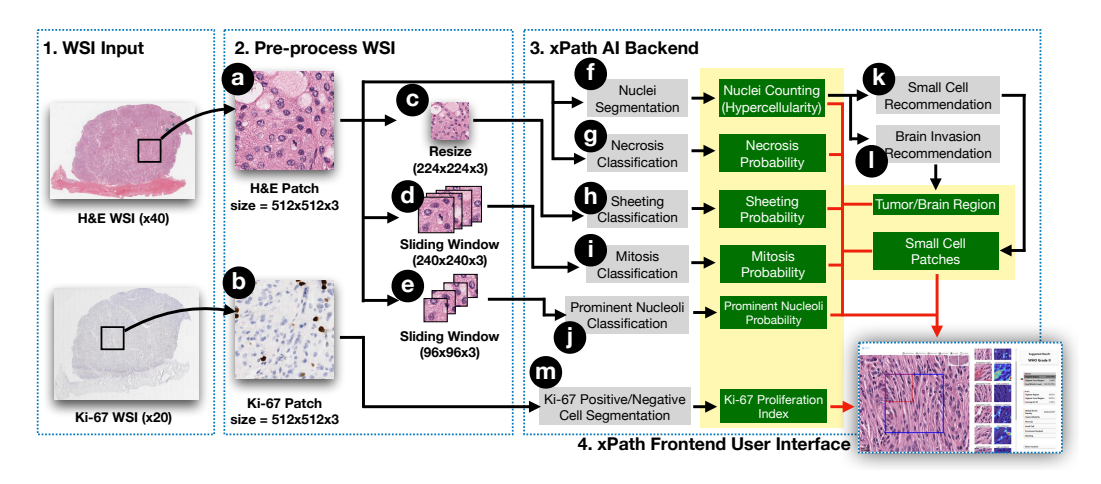


Fig. 7. Data processing pipeline of xPath: (i) xPath takes H&E and Ki-67 whole slide images (WSIs) as input. (ii) For each WSI, xPath uses a non-overlapping sliding window method to acquire (a) H&E and (b) Ki-67 patches (size=512 \times 512 \times 3); Furthermore, each 512 \times 512 \times 3 H&E patch is processed with (c) resizing, (d) sliding window (240 \times 240 \times 3), and (c) another sliding window (96 \times 96 \times 3) to fit the inputs of the down-stream models. (iii) xPath's AI backend takes over the pre-processed tiles and employs multiple AI models to detect WHO meningioma grading criteria from each patch. Given a 512 \times 512 \times 3 H&E patch, xPath uses (f) a nuclei segmentation model to count the number of nuclei (for hypercellularity judgment), (g) a necrosis classification model to calculate necrosis probability, and (h) a sheeting classification model to calculate sheeting probability. xPath further utilizes the nuclei counting results for (k) small cell recommendation, and (l) brain invasion recommendation. For a 240 \times 240 \times 3 tile, xPath uses (j) a prominent nucleoii classification model to obtain mitosis probability. For a 96 \times 96 \times 3 tile, xPath uses (j) a prominent nucleoii classification model to predict prominent nuclei probability. For each 512 \times 512 \times 3 Ki-67 patch, xPath detects positive and negative nucleus and calculates the Ki-67 proliferation index; (iv) All AI-computed results (marked in the green boxes) are shown in xPath's frontend for pathologist users to oversee.

distill quantized information on histological features. Below we describe how xPATH uses these techniques to process a whole slide image (WSI).

- 6.1.1 Pre-process whole slide images. Figure 7 shows a pipeline of how xPATH pre-processes a whole slide image. At first, xPATH cuts a high-resolution ($\sim (10^5)^2$) whole slide image into $512 \times 512 \times 3$ -pixel¹² patches with non-overlapping sliding windows. A patch with an average pixel value greater than 240 is considered as background and is discarded. Otherwise, xPATH further processes each patch separately to fit the tasks of detecting the eight criteria:
 - For the criteria of Ki-67 proliferation index, hypercellularity, necrosis, small cell, brain invasion, xPATH directly applies each AI model or detection rule to the patch;
 - For detecting sheeting patterns, xPATH resizes each patch to 224 × 224 × 3 to reduce the computation burden;
 - For counting the mitotic figures, xPATH further processes each patch using a 240 × 240 sliding window with a step size of 120 to fit the input of the mitosis classification model;
 - For counting prominent nucleolus, xPATH cuts each patch with a 96 × 96 non-overlapping sliding window to fit the prominent nucleoli classification model.

 $^{^{12}}$ For the criteria of sheeting and Ki-67 proliferation index, the dimension of each pixel is 0.5 μm . For other criteria, the dimension of each pixel is 0.25 μm .

6.1.2 Detecting each criterion with machine learning techniques. After XPATH pre-processes the whole slide image, it runs eight techniques to detect eight criteria, which covers three types of tasks: classification (to justify whether a given image is positive or not), semantic segmentation (to recognize and segment nucleus from the tissue background), and rule-based image recommendation¹³ (to recommend candidates based on fixed rules). Below we describe the target of each task and its formulation. Specific thresholds are justified by the maximum F1 scores achieved by each model in the validation set.

- Mitotic Count (Classification). xPATH uses an EfficientNet-b7 model [59] to identify mitosis (Figure 7i). A 240 × 240 tile with a prediction probability > 0.78 is counted as positive. xPATH further applies a non-maximum suppression technique to post-process the overlapping positive tiles. The mitotic distribution of the slide is calculated by merging the results from each 512 × 512 × 3 H&E patch.
- **Ki-67 Proliferation Index (Semantic Segmentation).** xPATH uses a pre-trained Cycle-GAN model [22] to detect both Ki-67 positive and negative nucleus (Figure 7m). Given a 512 × 512 × 3 Ki-67 patch as the observation region, the Ki-67 proliferation index is calculated as

 $\frac{\text{positive-count}}{\text{positive-count+negative-count}} \times 100\%.$

- Hypercelluarity (Semantic Segmentation). xPATH uses a pre-trained deep neural network [23] to segment and count the number of nuclei in a 512 × 512 × 3 H&E patch (Figure 7f).
- Necrosis (Classification). xPATH uses an EfficientNet-b5 model to justify whether a 512 × 512 × 3 H&E patch contains the necrosis pattern (Figure 7g). A patch is considered necrosis-positive if the prediction probability > 0.74.
- Small Cell (Rule-Based Recommendation). xPATH applies the rules for recognizing small cell patterns: selecting and recommending the top-10 512 × 512 × 3 H&E patches with the highest nuclei count within each slide (Figure 7k). For each recommended patch, if it has >125 nucleus/patch, then xPATH includes it in the recommendation.
- Prominent Nucleoli (Classification). Similar to mitosis classification, xPATH uses an EfficientNet-b0 model to classify prominent nucleoli (Figure 7j). To avoid false-positive cases influencing the result, only tiles that have >0.9 prediction probabilities are counted as positive ¹⁴. xPATH counts positive tiles in each 512 × 512 × 3 patch for calculating the distribution of prominent nucleoli.
- **Sheeting (Classification)**. xPATH uses an EfficientNet-b1 model [59] to classify whether the patch includes a sheeting pattern (Figure 7h). A sheeting patch is justified as positive if its prediction probability is >0.52.
- Brain Invasion (Classification). xPATH outlines the brain invasion pattern by classifying whether a given 512×512×3 H&E patch is tumor, brain, or background (Figure 7l). If the tumor cells are invading the normal brain tissues, it can be seen clearly with a heatmap visualization of tumors vs. brain areas. Because meningioma is a high-cellular tumor, xPATH classifies tumor patches with the following rule: (i) patches that have >55 nucleus in each H&E patch are counted as the tumor; (ii) patches that have [10,55] nucleus are counted as the brain; (iii) otherwise, count as the background.

 $[\]overline{^{13}}$ xPATH uses such an unsupervised approach to detect the small cell pattern because of a shortage of IRB-approved annotated data.

¹⁴We choose precision rather than recall in the prominent nucleoli classification because (*i*) the performance of the prominent nucleoli classification model is not satisfactory (see Section 6.3); (*ii*) unlike mitosis, this criterion is justified by the presence of cell *clusters* that have prominent nucleolus, and missing one or a few detections would not significantly influence the overall result.

Dataset	Dimension	# of Samples	# of Samples
	(in pixels)	(Training)	(Testing)
Mitosis Nuclei	240 × 240 × 3	33,562 (1,925 positive, 31,637 negative)	8,223 (336 positive, 7,887 negative)
Necrosis	512 × 512 × 3	4,383 (from 190 regions)	3,587 (from 162 regions)
		(651 positive, 3,732 negative)	(770 positive, 2,817 negative)
Prominent Nucleoli	96 × 96 × 3	15,042 (2,447 positive, 12,595 negative)	3,753 (609 positive, 3,144 negative)
Sheeting	224 × 224 × 3	3,660 (from 55 regions)	2,340 (from 45 regions)
		(1605 positive, 2055 negative)	(1,185 positive, 1,155 negative)

Table 1. Dataset descriptions for each task. The input patch dimension in pixels, the size of training/testing sets, and the distribution of positive/negative patches are provided.

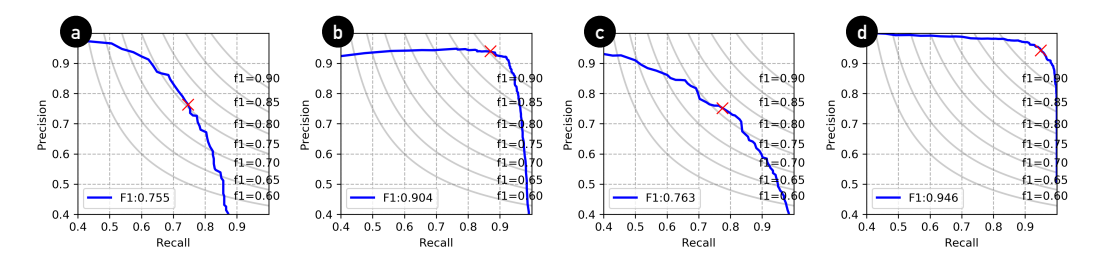


Fig. 8. Classification performance for (a) mitosis, (b) necrosis, (c) prominent nucleoli, (d) sheeting. The solid lines in each sub-figure illustrate the Precision-Recall curves of each model. The blue crosses indicate the performance achieved by the models using the thresholds that maximized the F1 scores on the validation sets.

6.2 Dataset and Model Training

We built an in-house dataset consisting of 30 WSIs from a local medical center for the model training and evaluation. The WSIs were cropped into patches of the expected dimensions for each model. For the supervised tasks, we created the ground-truth labels for all the patches by working with a board-certified neuropathologist. For the necrosis and sheeting patterns, we used a random-crop technique when generating patches from an annotated region. Note that patches in different sets were generated from a different group of regions. To train the models, we further randomly selected a subset of the training set to be the validation set, and utilized it to determine the optimal hyperparameters. Please find the supplementary material for more specific training details.

6.3 Technical Evaluation

We report the performance of AI models on testing sets. Specifically, we test the supervised models for recognizing mitosis, necrosis, prominent nucleoli, and sheeting criteria, and report the Precision-Recall curve, as shown in Figure 8. In summary, xPATH achieved F1 scores of 0.755, 0.904, 0.763, 0.946 in identifying the histological patterns of mitosis, necrosis, prominent nucleolus, and sheeting. The scores indicate the effectiveness of our models to implement xPATH. Moreover, for the tasks of cell-counting in hypercellularity and Ki-67 proliferation index criteria, we tested their performance with 150 randomly-selected $512 \times 512 \times 3$ patches each and report the average error rate. The results

show that the average error rate of nuclei counting (hypercellularity) and Ki-67 proliferation index is 12.08% and 29.36%, respectively.

Due to a lack of data at present, for brain invasion and small cell patterns, rather than drawing a definitive conclusion, xPATH uses a rule-based, unsupervised approach to recommend areas for pathologists to examine. We planned to validate the performance on these two criteria later in the work session with pathologists; however, it was hard for the participants to justify the small cell formation vs. inflammation areas without proper IHC tests. As such, xPATH's AI performance on detecting small cell patterns was not validated. For the brain invasion, most pathologists felt it was faster to examine it manually and did not rely on AI's recommendations.

7 WORK SESSIONS WITH PATHOLOGISTS

The technical evaluation reported in the previous session validated the effectiveness of xPath's AI backend in the in-house dataset. However, it remains unanswered whether xPath is beneficial to pathologist users in real clinical settings. Notably, many previous cases showed how easily AI models could break although they showed high accuracy in training/test data [35, 57]. To address these concerns, we conducted work sessions with 12 medical professionals in pathology across three medical centers and studied their behavior of grading meningiomas using a traditional interface — an open-source whole slide image viewer called ASAP¹⁵ and xPath. In this study, we referred to the traditional interface as system 1 and xPath as system 2 to avoid biasing of participants. The main research questions are:

RQ1: Can xPATH enable pathologists to achieve accurate diagnoses?

One reason of utilizing AI in xPath is because it can highlight ROIs of multiple histological patterns, freeing pathologists from examining the entire slide. However, it is still yet unclear whether introducing AI will have a positive or a negative effect on pathologists' diagnoses: On one hand, multiple previous work show that the introduction of human-AI collaboration improves pathologists' performance [12, 63]; On the other hand, due to the existing limitations in AI models' accuracy, users face the risk to generating wrong diagnoses if they over-rely on the non-perfect AI [7, 11]. As such, we hypothesize that -

• [H1] Pathologists' grading decisions with xPATH will be as accurate as those with manual examinations.

RQ2: Do pathologists work more efficiently with xPATH?

Another reason for using AI in xPath is that it can improve the pathologists' throughput by alleviating their workload. However, it remains unanswered how AI will assist pathologists in xPath, given that previous work shows less-carefully-designed AI might incur extra burdens [24]. As such, it is also necessary to find out whether pathologists can work efficiently with xPath's AI. We hypothesize that —

- [H2a] Pathologists will spend less time examining meningioma cases using XPATH.
- [H2b] Pathologists will perceive less effort using XPATH.

RQ3: Overall, does xPATH add value to pathologists' existing workflow?

Going beyond the influence brought by AI, we introduce two design ingredients — joint-analyses of multiple criteria *and* explanation by hierarchically traceable evidence — to fulfill the three system requirements (*i.e.*, comprehensiveness, explainability, integrability). In this study, we investigate whether such designs will add value to pathologists' existing workflow. Specifically, we hypothesize that:

¹⁵https://computationalpathologygroup.github.io/ASAP/. This tool was selected because it is open-source and has gained popularity in the digital pathology research domain [39].

- [H3a] XPATH will improve comprehensiveness with the joint-analyses of multiple criteria.
- [H3b] XPATH will improve explainability with explanation by hierarchically traceable evidence.
- [H3c] xPATH will improve integrability with the top-down human-AI collaboration workflow.

7.1 Participants

We recruited 12 medical professionals in pathology across three medical centers. Our participants' experience ranged from two to 10 years (μ =4.38, σ =2.16), including two attendings (A), two fellows (F), seven senior residents (SR, \geq PGY-3), and one junior resident (JR, \leq PGY-2)¹⁶. All participants had received training for examining meningiomas prior to the work session. Regarding familiarity with digital pathology tools, pathologists had more experience in glass slides than interfaces in digital pathology: six of them used ImageScope¹⁷ occasionally for training or reviewing remote cases.

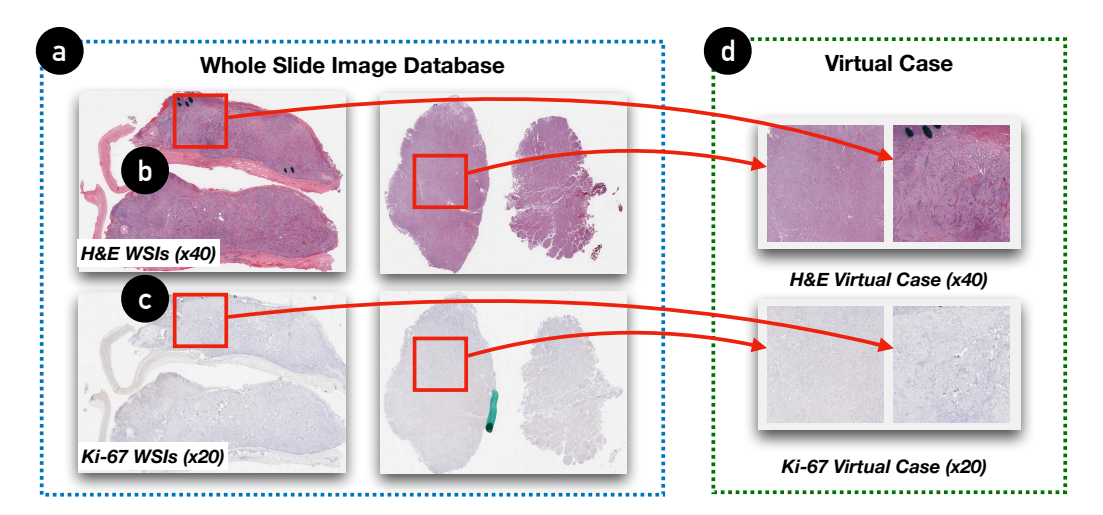


Fig. 9. We used the 'virtual cookie cut' technique to generate the tests cases. Specifically, we first collected (a) pairs of H&E (in x400) and Ki-67 (in x200) WSIs from a local medical center. Then, we generated 'virtual cuts' by (b) selecting $30,000\times30,000$ -pixel regions in H&E WSIs, and (c) $15,000\times15,000$ -pixel regions from the same position as their H&E counterparts. (d) Each virtual case consists of one mandatory H&E slide with two nodes and one optional Ki-67 slide with two corresponding ones.

7.2 Test Data

We collected 18 IRB-approved meningioma WSIs¹⁸ from the same medical center to generate the test cases. In normal conditions, each patient's case consisted of more than 10 WSIs, and an averaged-experienced resident pathologist typically needs to spend about one hour to finish examining an averaged-difficult case (*i.e.*, criteria found in the case do not lie on the grading borderlines). As such, we generated nine 'virtual cases' with the 'virtual cookie cut' technique (see Figure 9) to fit

¹⁶Please see the supplementary material for the demographic information for the participants.

¹⁷https://www.leicabiosystems.com/digital-pathology/manage/aperio-imagescope/

¹⁸...which include eleven H&E WSIs (scanned in x400), and seven Ki-67 WSIs (scanned in x200).

the task of grading meningiomas¹⁹ into the hour-long work sessions. Each virtual case consists of a mandatory H&E slide (in x400), and an optional Ki-67 slide (in x200). Each H&E slide consists of two nodes (each has a size of 30,000×30,000, which is relatively smaller than the real cases), while each Ki-67 slide has two corresponding Ki-67 nodes (each has a size of 15,000×15,000) that were cut from the same position as their H&E counterparts, if available. In total, nine virtual cases have nine H&E slides and six Ki-67 slides, *i.e.*, three virtual cases do not come with a corresponding Ki-67 slide. As for the ground-truth grading diagnosis, 2/9 is grade I, 5/9 is grade II, and 2/9 is grade III. We selected three from the grade II cases for the tutorial purpose for the work session, leaving the test set with two cases for each grade.

7.3 Task & Procedure

All sessions were conducted online because of the COVID-19 pandemic. We first introduced the mission of the project and provided a detailed walkthrough of the traditional interface and xPATH with three pairs of H&E and Ki-67 slides as an example. Participants used Microsoft Remote Desktop to interact with both systems that ran on a remote server. After that, we ran a testing session for the participants to grade one virtual case with the traditional interface, and one-four other virtual cases with xPATH with the time cost logged²⁰. The order was counterbalanced across participants. For each case, the time was counted from when participants first clicked the WSI case until they reached the grading diagnosis. After participants finished each case, we asked them to report their grading diagnosis as well as their findings through a questionnaire adapted from the College of American Pathologists (CAP) cancer protocol template²¹. In this session, we did not compare xPATH with traditional optical microscopes because of the difficulty of instrumentation and observation given the remote situation. After participants had examined all the cases, we conducted a semi-structured interview to elicit their responses to xPATH's perceived effort and added value. The average duration of each work session was ~70 minutes. Each participant was paid with a \$100 gift card as compensation for their time.

7.4 Measurements

In this study, we collected participants' grading decisions from the CAP questionnaire and analyzed the time log. We also asked them to fill in a post-study questionnaire (see Table 2) with seven-point Likert questions following [13, 26, 34]. We tested our hypotheses via the following measurements:

For **H1**, we compared the gradings reported by participants and the 'ground-truth' gradings provided by a board-certified neuropathologist. We measured the accuracy of both systems by calculating the error rates of gradings.

For **H2a**, we calculated the average time participants spent on each case using xPATH and the traditional interface. For **H2b**, we asked them to give both systems ratings to the effort needed for grading (Table 2, W1), and the effect of the system to reduce the workload (Table 2, W2) in the post-study questionnaire.

H3a-c was evaluated by the post-study questionnaire. For **H3a**, we asked participants to rate the comprehensiveness of хРатн and the traditional interface (Table 2, C1). For **H3b**, we asked them to rate the explainability of хРатн only since the traditional interface did not provide AI detections (Table 2, E1). For **H3c**, we asked participants to rate the integrability of both systems (Table 2, I1).

 $^{^{19}}$ We would like to point out that all cases used in this study are meningioma-positive. Pathologists' task was to *grade* meningiomas instead of justifying each case as positive vs. negative.

²⁰Variation in the number of cases in xPath was caused by the difference in the participants' ability. Details of the arrangement are reported in the supplementary material.

²¹https://documents.cap.org/protocols/cp-cns-18protocol-4000.pdf

Apart from the hypotheses, we further investigated whether the participants trusted xPATH by asking them the following two questions: (*i*) How capable is the system at helping grade meningiomas? (Table 2, T1), (*ii*) How confident do you feel about the accuracy of your diagnoses using the system? (Table 2, T2). We also studied whether the participants would like to use both systems in the future (Table 2, F1), and also let the participants to rate the overall preference of system 1 vs. system 2 (Table 2, F2).

8 RESULTS & FINDINGS

In this section, we first discuss our initial research questions and hypotheses. Then, we summarize the recurring themes that we have found in the working sessions.

8.1 RQ1: Can XPATH enable pathologists to achieve accurate diagnoses?

We summarize the CAP questionnaire responses from our participants and collect 12 grading decisions from the traditional interface, and 20 from xPATH. We then follow previous works on digital histology [56, 61] and compare the difference between pathologists' responses and the ground truth diagnoses justified by a board-certified neuropathologist. In summary, with the traditional interface, participants gave correct gradings for 7/12 cases, lower-than-ground-truth gradings for 4/12 cases, and higher-than-ground-truth grading for 1/12 case. In comparison, using xPATH, pathologists gave 17/20 cases correct gradings and lower-than-ground-truth gradings in 3/20 diagnoses. Upon further analysis, we found that all three errors that participants made with xPATH were caused by their over-reliance on the AI. In these cases specifically, participants spent their majority of effort examining the evidence reported by xPATH and missed the false-negative features that xPATH failed to detect —

It's just that I got caught up in looking at the boxes and I would forget that I should look at the entire case myself. (P4)

In sum, based on the data collected by the study, we report that pathologists could make more accurate grading decisions with xPATH in comparison to the traditional interface (**H1**).

8.2 RQ2: Do pathologists work more efficiently with xPATH?

Contrary to our hypothesis (**H2a**), participants spent an average of 7min13s examining each case using xPath, which is 1min17s higher than the traditional interface (ASAP). Our study suggests that pathologists tended to (p=0.050) invest more time in xPath than the traditional interface. We believe this is partly because xPath brings pathologists an extra workload to comprehend and oversee the AI findings. In the traditional interface, our participants share a similar workflow of examining the WSI — they first scanned the entire WSI in low magnification, then prioritized studying one criterion (such as the brain invasion or the mitotic count) to ascertain a probable diagnosis as quickly as possible. They also checked Ki-67 slides to assist the diagnosis. In this process, they collected evidence that accounts for a higher grade and memorized them in their minds. Once they acquired enough evidence, they would stop and make a grading decision. When using xPath, participants did not abandon their standard workflow as in the traditional interface. Rather, on top of their standard workflow, participants would perform the differential diagnosis based on AI's findings — they clicked through each piece of evidence in xPath, justified it by registering into the WSI, and at times overrode AI by clicking the approve/decline/declare-uncertain buttons. These extra steps of interactions prolong participants' workflow —

System 2 (xPath) actually makes it longer because some of the images have sort of competing opinions — whether this is mitosis or not ... So I'd better take a closer look at what the machine suggests. (P3)

Question		хРатн	
C1: Rate the comprehensiveness of the system.		5.75(0.75)	
E1: Rate the explainability of the system.		5.58(0.90)	
I1: Rate the integrability of the system.		5.91(1.08)	
W1: Rate the effort needed to grade meningiomas when using the system.		0.91(0.90)	
W2: Rate the effect of the system on your workload to reach a diagnosis.		5.83(1.03)	
T1: How capable is the system at helping grade meningiomas?		5.83(0.94)	
T2: How confident do you feel about the accuracy of your diagnoses using the system?		6.00 (0.95)	
F1: If approved by the FDA, I would like to use this system in the future.		6.42(0.79)	
F2: Overall preference		6.75(0.45)	

Table 2. Participant response on the quantitative measurements of a traditional interface (ASAP) and XPATH with seven-point Likert scores. For the rating questions (C1, E1, I1, W1, W2), 1=lowest and 7=highest. For question T1, T2, F1, 1=very strongly disagree, 2=strongly disagree, 3=slightly disagree, 4=neutral, ..., and 7=very strongly agree. For question F2, score 1=totally prefer system 1 over system 2, 2=much more prefer system 1 over system 2, 3=slightly prefer system 1 over system 2, 4=neutral, ..., and 7=very strongly prefer system 2 over system 1. Note that for question W1, a higher rating indicates users perceive more effort while using the system. Question E1, T1, T2 are not applicable to ASAP, since it does not have AI detections for users.

Regarding the perceived effort (**H2b**), participants reported significantly less effort (as shown in Table 2, W1, xPath: μ =0.91, ASAP: μ =3.67, p=0.002) and a stronger effect on reducing the workload (Table 2, W2, xPath: μ =5.83, ASAP: μ =2.17, p=0.002) while using xPath. Pathologists mentioned that automating the process of finding small-scaled histological features, especially mitosis, would save their time and effort —

I spend a lot more time crawling around the slide in the high-power looking for mitosis (for system 1), which you don't have to do as much in system 2 (xPATH). (P8)

8.3 RQ3: Overall, does xPATH add value to pathologists' existing workflow?

For the comprehensiveness dimension (H3a), xPath received a significantly higher rating than the traditional interface (Table 2, C1, xPath: μ =5.75, ASAP: μ =2.83, p=0.001). Specifically, pathologists responded positively that xPath provides sufficient information (*i.e.*, criteria and evidence) to assist the diagnosis —

...it (хРАТН) kind of gives you a step-wise checklist to make sure that it's the correct diagnosis, and also provides you what is most likely a diagnosis. (P11)

For the explainability dimension (H3b), xPath obtained an average rating of 5.58/7 (Table 2, E1). In general, pathologists could understand the logical relationship between the evidence and the suggested grading (global explainability). However, some (P1, P5) found it hard to interpret the saliency map, especially for the cases where cues of attentions scattered across the entire evidence (see Figure 11a) -

For the heatmap ... it is also a little bit confusing ... it takes some time getting used to it and there are some false positives. (P1)

For the integrability dimension (**H3c**), pathologists gave overall higher scores for xPATH (Table 2, I1, xPATH: μ =5.91, ASAP: μ =4.17, p=0.006). Specifically, pathologists were able to perform diagnoses based on the xPATH's AI findings similar to their workflow of collaborating with human trainees —

It's kind of like a first-year resident marking everything. (P1)

I'm a cytology fellow, and cases are pre-screened for us. And essentially this is doing similarly. (P4)

For the trust dimension, participants responded positively to xPath's capability of helping to grade meningiomas (T1: μ =5.83) and the accuracy of the diagnoses while using the system (T2: μ =6.00). However, some (P3, P4, P5) pointed out that they might spend more time examining the WSI entirely if more time had been granted —

I just went to the areas that the system suggested. If I had more time, I would like to just go to all the areas, just to feel more comfortable that I'm not missing anything. (P5)

Last but not least, participants were more likely to use xPATH than the traditional interface (Table 2, F1, xPATH: μ =6.41, ASAP: μ =3.75, p=0.002). Overall, 9/12 of the participants "totally" preferred xPATH over the traditional interface, while 3/12 "much more" preferred xPATH (Table 2, F2).

However, it is noteworthy that this study is based on pathologists' examination of WSIs, while pathologists use the optical microscope in their daily practice. During the study, 7/12 of our participants expressed that they preferred using an optical microscope with the glass slide *vs.* a digital interface with the WSI — "... it's much faster (in the microscope) than moving on the computer ... we would prefer to look at a real slide instead of using a scan picture." (P2). As such, further comparison between xPATH and the optical microscope is considered as future work.

8.4 Recurring Themes

Based on our observations of pathologists' using xPATH and the interview with them, we discuss the following recurring themes that characterize how pathologists interacted with xPATH.

8.4.1 How pathologists use XPATH's multiple criteria: prioritizing one, referring to others on-demand. We noted that pathologists tended to focus on a specific criterion. If that criterion alone did not meet the bar of a diagnosis for a higher grade, pathologists would use XPATH to browse other criteria, looking for evidence of a differential diagnosis, until they identify sufficient evidence to support their hypothesis.

I'm done. Because with the mitosis that high, you're done, you don't have to go through that stuff (other criteria). (P12)

However, some pathologists would also like to see other criteria and examine the slide comprehensively -

With the mitosis rate that high, you don't actually need it (Ki-67) for the diagnosis. But I will have a look at it. (P1)

I will just look at (other criteria) because I don't want to grade by one single criterion (mitosis). (P3)

Such a relationship between criteria is analogous to 'focus + context' [15] in information visualization — different pathologists might focus on a few different criteria. Still, the other criteria are also important to serve as context at their disposal to support an existing diagnosis or find an alternative.

8.4.2 xPATH's top-down workflow with hierarchical explainable evidence enables pathologists to navigate between high-level AI results & low-level WSI details. One of the main reasons limiting the throughput of histological diagnosis is that criteria like mitotic count have very small-scaled

histological features. As a result, pathologists have to switch to high power magnification to examine such small features in detail. Given the high resolution of the WSI, it is possible to 'get lost' in the narrow scope of HPF, resulting in a time-consuming process to go through the entire WSI. With xPATH, pathologists found its hierarchical design and the provision of mid-level evidence (e.g., AI's ROI samples) the most helpful for diagnosis as it connects high-level findings and low-level details —

It (xPATH) finds the best area to look at.... You can jump there, and if it is a grade III, then it is a grade III. You don't have to look at other areas. (P6)

Furthermore, pathologists appreciated that xPath provided heatmap visualizations to assist them in navigating the WSI out of the ROI samples -

The heatmap is very useful to assist pathologists to go through the entire slide ... which saves time and makes sure not missing anything. (P12)

8.4.3 xPATH's explainable design helps pathologists see what AI is doing. We found xPATH's evidence-based justification of AI findings assisted pathologists to relate AI-computed results with evidence, which added explainability —

System 2 (xPATH) does find some evidence and assigns it to a particular observation that is related to the grading, so that it helps with explainability. (P3)

In xPath, the AI might make two kinds of mistakes that may incur potential bias: (i) false positive, where AI mistakenly identifies negative areas as positive for a given criterion; (ii) false negative, where the AI misses positive areas corresponding to a criterion. We observed a number of false-positive detections that confused some participants. We also found out that the participants would rather deal with more false positives than false negatives so that signs of more severe grade would not be missed —

It's better that it picks them up and gives me the opportunity to decline it. (P10)

Furthermore, although some participants found the saliency map hard to interpret in some cases, the others used it to locate the cells that led to AI's grading —

There were a couple of instances where it was a bit more difficult to figure out what it (the saliency map) was trying to point out to me. But for the majority of the time, I could tell which area they (the saliency maps) were trying to show me. (P9)

Further, with the aid of the saliency map, participants could understand AI's limitations and what might have misled the AI -

You can see what this system counted as mitosis ... the heatmap (the saliency map) helps to understand why AI chose this or that area, for example, I think AI chose neutrophils as mitotic figures in some areas. (P6)

8.4.4 How pathologists oversee XPATH: incrementing human findings onto justified AI results. Given the explainable evidence provided by xPATH, it was straightforward for pathologists to recognize and modify AI results when there was a disagreement. Specifically, pathologists could oversee AI by clicking on the approve/decline/declare-uncertain buttons or modifying AI results directly on the criteria panel. If the overseen AI result were sufficient to conclude a grading decision (e.g., seven mitoses in 10 HPFs, enough to make the case as grade II (>4), but still far from grade III («20)), they would stop examining and report the grading. However, if the overseen AI result appeared to be marginal (e.g., 19 mitoses in 10 HPFs, which is only one mitosis away from upgrading the case to a grade III), pathologists would continue to search based on the AI findings and add their new insights to grade —

I count a total of number of five ... adding previous 19 makes it 24 ... this is grade III. (P2)

What's more, for the cases where xPATH did not actively report positive detections, pathologists would examine the WSI manually as in a traditional interface — that is, pathologists would use their experience to evaluate the case further and make a grading decision.

9 LIMITATIONS, DESIGN RECOMMENDATIONS & FUTURE WORK

9.1 Limitations & Future Works

In this section, we discuss limitations of this work and outline the possible directions of future works.

9.1.1 Increasing the scope of study. One limitation of this work is the materials used. Specifically, we used the data from one institute to train and test the AI of xPATH. This leaves the performance of xPATH's AI questionable while applying the AI to the WSIs from other institutes. This is because other institutes might use a different staining process or a different type of scanner, causing a difference in the domain/distribution (see Figure 10).

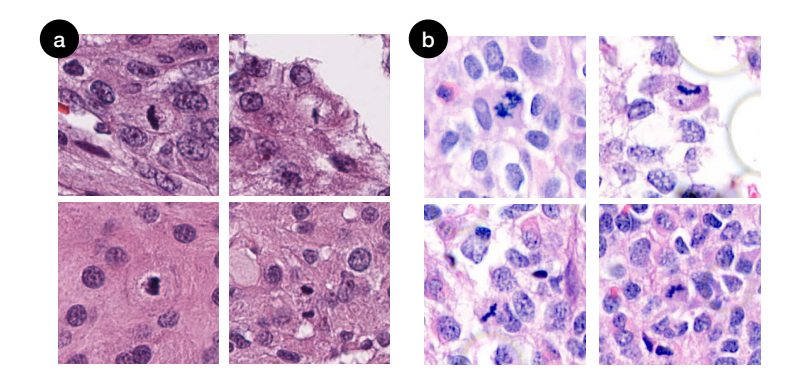


Fig. 10. Mitoses from meningiomas (in x400), scanned by (a) the medical center in this study and (b) a different medical center. The difference in appearance is caused by the difference in processing procedures and scanners used.

Another limitation is from the whole slide images. During the work sessions, more than half of the participants expressed that they preferred using an optical microscope with the glass slide vs. a digital interface with the WSI. Remarkably, participants found it challenging to navigate a digital WSI, which has also been described and discussed by Ruddle & Thomas $et\ al.$ [51]. We believe such a difficulty in navigation is partly related to the pathologists' unfamiliarity with the traditional (digital) interface. As such, we suggest future work also compare with the optical microscope aside from the traditional digital interface. Therefore, with more data points collected, we can validate xPATH's performance and the generalizability more comprehensively.

9.1.2 Enabling adjusting the thresholds in the frontend. Currently, хРАТН does not support directly adjusting the threshold on the frontend. In our user study, one participant mentioned that different pathologists might have different thresholds to justify whether a piece of evidence is positive —

"I only call the characteristic mitoses ... other pathologists might have different thresholds. (P7)

Further, dealing with false positives and false negatives is another issue with the fixed-threshold scheme. From our study, we found out that pathologists would prefer high-sensitivity results that include some false positives rather than high-specificity results that have false negatives —

I could have more faith if it could find all the candidates. And I could pretty easily click through and accept/reject, and know that it wasn't missing anything. (P8)

Therefore, the system by default should be designed to err on the side of caution, *e.g.*, showing a wide range of ROIs despite that some are inevitably false positives. Pathologists are fast in examining ROIs (and ruling out false positives), whereas missing important features would come with a much higher cost (*e.g.*, delayed or missed treatment).

9.1.3 Improving the quality and granularity of explanations. In the study, we found a number of cases where the saliency maps failed to explain the detection results and caused confusion to the users. As shown in Figure 11, the failed saliency maps showed either scattered attention across the evidence (Figure 11a), or concentrated attention at a wrong place (Figure 11b). Such errors can be explained as the attentions are reasoned from patch-wise annotations rather than localized ones because the localized annotations of positive findings are extremely labor-costly to obtain. The quality of the saliency maps can be potentially improved with the increment of training data for higher model generalization and the advent of the methodologies of unsupervised attention reasoning [4].

Besides, knowing the location of a potential positive finding can be insufficient for pathologists. Since the pathological imaging of tissues is merely an approximation of the real condition, there can often exist uncertainty in diagnosis even for well-trained pathologists. As such, explaining why an area contains positive findings, *e.g.*, a highlighted cell is detected to stage as mitosis since its boundary is jagged, can be critical for systems in the future. Such causality enables a system to imitate how pathologists discuss with their peers, which can improve the collaboration between a system and its users. Moreover, future work should also employ more formal measurements (*e.g.*, System Causability Scale [28]) to evaluate the quality of explanations.

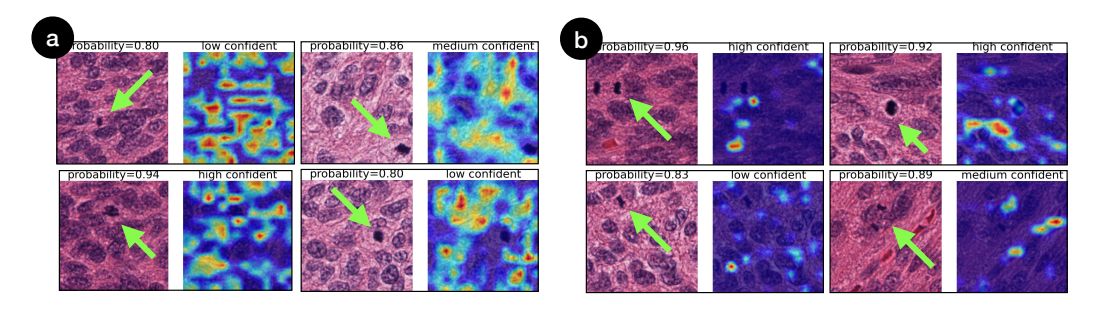


Fig. 11. Examples of failure explanation cases, where the saliency shows (a) scattered attentions across the image or (b) misleading hot spots. The green arrows point to the location of a mitosis figure marked by a human pathologist.

9.2 Design Recommendations for Physician-Al Collaborative Systems

9.2.1 Showing the logical relationship amongst multiple types of evidence at the top level. Carcinoma grading usually involves examining multiple criteria from multiple data sources (e.g., H&E slides, IHC slides, FISH (fluorescence in situ hybridization) test, patient's health record). As such, one-size-fits-all AI models are not sufficient. In practice, multiple AI models are employed to locate different types of disease markers. To organize these AI-computed results, medical AI systems (such as xPATH) should seek to present the logical relationship that connects these multiple criteria/features/sources of information and update final results dynamically given any pathologists'

input (*e.g.*, acceptance or rejection of how AI computes each criterion). Such a design is more likely to match the clinical practice of pathologists and cost minimal extra learning when users onboard a system. It is noteworthy that the 'multiple criteria' design is not limited to this research but can also generalize to other tasks in digital pathology, such as breast cancer grading [49].

- 9.2.2 Making AI's finding traceable with hierarchically organized evidence. There is a pressing need to deal with the transparency of a black-box model and the traceability of the explanation evidence in the high-stake tasks (e.g., medical diagnosis). As such, AI systems should provide local explainability where each piece of low-level evidence is traceable. In xPATH, we employ the design of hierarchically traceable evidence for each criterion. Such an organization forms an 'evidence chain' where each direct evidence is accountable for the high-level system output. Similar intuitions can also be applied to medical applications in a more general context, such as cancer staging [43] and cancer scoring [32], where the evidence is accumulated to arrive at a diagnosis.
- 9.2.3 Employing a focus+context design towards presenting and/or interacting with multiple criteria. Medical diagnosis involves accumulating evidence from multiple criteria our study observed that pathologists started with focusing on one criterion while continuing to examine the others for a differential diagnosis. Thus, medical AI systems should make multiple criteria available, and support the navigation of such criteria following a 'focus+context' design [15], which is commonly used in information visualization. The major design goal is to strike the dichotomy between juxtaposing the focused criterion with sufficient contextual criteria and overwhelming the pathologists with too much information. It is also possible for a system to, based on a patient's prior history and the pre-processing of their data, recommend a pathologist to start focusing on specific criteria followed by examining some others as context.

10 CONCLUSION

In this work, we identify three gaps of comprehensiveness, explainability, and integrability that prevent AI from being adopted in a clinical setting for pathologists. To close these gaps, we implement xPATH with two key design ingredients: (i) joint-analyses of multiple criteria and (ii) explanation by hierarchically traceable evidence. To validate xPATH, we conducted work sessions with twelve medical professionals in pathology across three medical centers. Our findings suggest that xPATH can leverage AI to reduce pathologists' cognitive workload for meningioma grading. Meanwhile, pathologists learned the tool and benefited from the design (e.g., working with multiple criteria in parallel while drilling down to more evidence for individual criteria), and made fewer mistakes. By observing pathologists' use of xPATH with quantitative and qualitative feedback, we shed light on how pathologists collaborate with AI and summarize design recommendations. We believe this work can help future research on tool design for physician-AI collaborative diagnosis.

REFERENCES

- [1] Ellen Abry, Ingrid Ø Thomassen, Øyvind O Salvesen, and Sverre H Torp. 2010. The significance of Ki-67/MIB-1 labeling index in human meningiomas: a literature study. *Pathology-Research and Practice* 206, 12 (2010), 810–815.
- [2] Saleema Amershi, Dan Weld, Mihaela Vorvoreanu, Adam Fourney, Besmira Nushi, Penny Collisson, Jina Suh, Shamsi Iqbal, Paul N Bennett, Kori Inkpen, et al. 2019. Guidelines for human-AI interaction. In Proceedings of the 2019 CHI Conference on Human Factors in Computing Systems. ACM, 3.
- [3] Vahid Anari, Parvin Mahzouni, and Rasoul Amirfattahi. 2010. Computer-aided detection of proliferative cells and mitosis index in immunohistichemically images of meningioma. In 2010 6th Iranian Conference on Machine Vision and Image Processing. IEEE, 1–5.
- [4] Alejandro Barredo Arrieta, Natalia Díaz-Rodríguez, Javier Del Ser, Adrien Bennetot, Siham Tabik, Alberto Barbado, Salvador García, Sergio Gil-López, Daniel Molina, Richard Benjamins, et al. 2020. Explainable Artificial Intelligence (XAI): Concepts, taxonomies, opportunities and challenges toward responsible AI. *Information Fusion* 58 (2020), 82–115.

[5] Thomas Backer-Grøndahl, Bjørnar H Moen, and Sverre H Torp. 2012. The histopathological spectrum of human meningiomas. *International journal of clinical and experimental pathology* 5, 3 (2012), 231.

- [6] Peter Bankhead, Maurice B Loughrey, José A Fernández, Yvonne Dombrowski, Darragh G McArt, Philip D Dunne, Stephen McQuaid, Ronan T Gray, Liam J Murray, Helen G Coleman, et al. 2017. QuPath: Open source software for digital pathology image analysis. Scientific reports 7, 1 (2017), 16878.
- [7] Gagan Bansal, Besmira Nushi, Ece Kamar, Walter S Lasecki, Daniel S Weld, and Eric Horvitz. 2019. Beyond accuracy: The role of mental models in human-AI team performance. In *Proceedings of the AAAI Conference on Human Computation and Crowdsourcing*, Vol. 7. 2–11.
- [8] Jocelyn Barker, Assaf Hoogi, Adrien Depeursinge, and Daniel L Rubin. 2016. Automated classification of brain tumor type in whole-slide digital pathology images using local representative tiles. Medical image analysis 30 (2016), 60–71.
- [9] Kaustav Bera, Kurt A Schalper, David L Rimm, Vamsidhar Velcheti, and Anant Madabhushi. 2019. Artificial intelligence in digital pathology—new tools for diagnosis and precision oncology. *Nature reviews Clinical oncology* 16, 11 (2019), 703–715.
- [10] Daniel J Brat, Joseph E Parisi, Bette K Kleinschmidt-DeMasters, Anthony T Yachnis, Thomas J Montine, Philip J Boyer, Suzanne Z Powell, Richard A Prayson, and Roger E McLendon. 2008. Surgical neuropathology update: a review of changes introduced by the WHO classification of tumours of the central nervous system. Archives of pathology & laboratory medicine 132, 6 (2008), 993–1007.
- [11] Zana Buçinca, Maja Barbara Malaya, and Krzysztof Z Gajos. 2021. To trust or to think: cognitive forcing functions can reduce overreliance on AI in AI-assisted decision-making. *Proceedings of the ACM on Human-Computer Interaction* 5, CSCW1 (2021), 1–21.
- [12] Wouter Bulten, Maschenka Balkenhol, Jean-Joël Awoumou Belinga, Américo Brilhante, Aslı Çakır, Lars Egevad, Martin Eklund, Xavier Farré, Katerina Geronatsiou, Vincent Molinié, et al. 2021. Artificial intelligence assistance significantly improves Gleason grading of prostate biopsies by pathologists. *Modern Pathology* 34, 3 (2021), 660–671.
- [13] Carrie J Cai, Emily Reif, Narayan Hegde, Jason Hipp, Been Kim, Daniel Smilkov, Martin Wattenberg, Fernanda Viegas, Greg S Corrado, Martin C Stumpe, et al. 2019. Human-centered tools for coping with imperfect algorithms during medical decision-making. In Proceedings of the 2019 CHI Conference on Human Factors in Computing Systems. 1–14.
- [14] Carrie J Cai, Samantha Winter, David Steiner, Lauren Wilcox, and Michael Terry. 2019. "Hello AI": Uncovering the Onboarding Needs of Medical Practitioners for Human-AI Collaborative Decision-Making. *Proceedings of the ACM on Human-computer Interaction* 3, CSCW (2019), 1–24.
- [15] Mackinlay Card. 1999. Readings in information visualization: using vision to think. Morgan Kaufmann.
- [16] Anne E Carpenter, Thouis R Jones, Michael R Lamprecht, Colin Clarke, In Han Kang, Ola Friman, David A Guertin, Joo Han Chang, Robert A Lindquist, Jason Moffat, et al. 2006. CellProfiler: image analysis software for identifying and quantifying cell phenotypes. *Genome biology* 7, 10 (2006), R100.
- [17] Aditya Chattopadhay, Anirban Sarkar, Prantik Howlader, and Vineeth N Balasubramanian. 2018. Grad-cam++: Generalized gradient-based visual explanations for deep convolutional networks. In 2018 IEEE winter conference on applications of computer vision (WACV). IEEE, 839–847.
- [18] Xiang'Anthony' Chen, Ye Tao, Guanyun Wang, Runchang Kang, Tovi Grossman, Stelian Coros, and Scott E Hudson. 2018. Forte: User-driven generative design. In Proceedings of the 2018 CHI Conference on Human Factors in Computing Systems. 1–12.
- [19] Alberto Corvo, Marc A van Driel, and Michel A Westenberg. 2017. PathoVA: A visual analytics tool for pathology diagnosis and reporting. In 2017 IEEE Workshop on Visual Analytics in Healthcare (VAHC). IEEE, 77–83.
- [20] Pat Croskerry, Karen Cosby, Mark L Graber, and Hardeep Singh. 2017. Diagnosis: Interpreting the shadows. CRC Press.
- [21] Soumya De, R Joe Stanley, Cheng Lu, Rodney Long, Sameer Antani, George Thoma, and Rosemary Zuna. 2013. A fusion-based approach for uterine cervical cancer histology image classification. *Computerized medical imaging and graphics* 37, 7-8 (2013), 475–487.
- [22] Parmida Ghahremani, Yanyun Li, Arie Kaufman, Rami Vanguri, Noah Greenwald, Michael Angelo, Travis J Hollmann, and Saad Nadeem. 2021. DeepLIIF: Deep Learning-Inferred Multiplex ImmunoFluorescence for IHC Image Quantification. bioRxiv (2021).
- [23] Simon Graham, Quoc Dang Vu, Shan E Ahmed Raza, Ayesha Azam, Yee Wah Tsang, Jin Tae Kwak, and Nasir Rajpoot. 2019. Hover-net: Simultaneous segmentation and classification of nuclei in multi-tissue histology images. Medical Image Analysis (2019), 101563.
- [24] Hongyan Gu, Jingbin Huang, Lauren Hung, and Xiang'Anthony' Chen. 2020. Lessons learned from designing an AI-enabled diagnosis tool for pathologists. arXiv preprint arXiv:2006.12695 (2020).
- [25] Grzegorz T Gurda, Alexander S Baras, and Robert J Kurman. 2014. Ki-67 index as an ancillary tool in the differential diagnosis of proliferative endometrial lesions with secretory change. *International Journal of Gynecological Pathology* 33, 2 (2014), 114–119.

- [26] Sandra G Hart and Lowell E Staveland. 1988. Development of NASA-TLX (Task Load Index): Results of empirical and theoretical research. In *Advances in psychology*. Vol. 52. Elsevier, 139–183.
- [27] Narayan Hegde, Jason D Hipp, Yun Liu, Michael Emmert-Buck, Emily Reif, Daniel Smilkov, Michael Terry, Carrie J Cai, Mahul B Amin, Craig H Mermel, et al. 2019. Similar image search for histopathology: SMILY. *NPJ digital medicine* 2, 1 (2019), 1–9.
- [28] Andreas Holzinger, André Carrington, and Heimo Müller. 2020. Measuring the quality of explanations: the system causability scale (SCS). KI-Künstliche Intelligenz (2020), 1–6.
- [29] Andreas Holzinger, Bernd Malle, Peter Kieseberg, Peter M Roth, Heimo Müller, Robert Reihs, and Kurt Zatloukal. 2017. Towards the augmented pathologist: Challenges of explainable-ai in digital pathology. arXiv preprint arXiv:1712.06657 (2017).
- [30] Eric Horvitz. 1999. Principles of mixed-initiative user interfaces. In *Proceedings of the SIGCHI conference on Human Factors in Computing Systems.* 159–166.
- [31] Yongxiang Huang and Albert Chi-shing Chung. 2018. Improving high resolution histology image classification with deep spatial fusion network. In *Computational Pathology and Ophthalmic Medical Image Analysis*. Springer, 19–26.
- [32] Peter A Humphrey. 2004. Gleason grading and prognostic factors in carcinoma of the prostate. Modern pathology 17, 3 (2004), 292–306.
- [33] Humayun Irshad. 2013. Automated mitosis detection in histopathology using morphological and multi-channel statistics features. *Journal of pathology informatics* 4 (2013).
- [34] Patrick W Jordan, Bruce Thomas, Ian Lyall McClelland, and Bernard Weerdmeester. 1996. *Usability evaluation in industry*. CRC Press.
- [35] Sasikiran Kandula and Jeffrey Shaman. 2019. Reappraising the utility of Google flu trends. PLoS computational biology 15, 8 (2019), e1007258.
- [36] Daisuke Komura and Shumpei Ishikawa. 2018. Machine learning methods for histopathological image analysis. *Computational and structural biotechnology journal* 16 (2018), 34–42.
- [37] Robert Krueger, Johanna Beyer, Won-Dong Jang, Nam Wook Kim, Artem Sokolov, Peter K Sorger, and Hanspeter Pfister. 2019. Facetto: Combining unsupervised and supervised learning for hierarchical phenotype analysis in multi-channel image data. IEEE transactions on visualization and computer graphics 26, 1 (2019), 227–237.
- [38] Bokyung Lee, Taeil Jin, Sung-Hee Lee, and Daniel Saakes. 2019. SmartManikin: Virtual Humans with Agency for Design Tools. In *Proceedings of the 2019 CHI Conference on Human Factors in Computing Systems*. 1–13.
- [39] Geert Litjens, Peter Bandi, Babak Ehteshami Bejnordi, Oscar Geessink, Maschenka Balkenhol, Peter Bult, Altuna Halilovic, Meyke Hermsen, Rob van de Loo, Rob Vogels, et al. 2018. 1399 H&E-stained sentinel lymph node sections of breast cancer patients: the CAMELYON dataset. GigaScience 7, 6 (2018), giy065.
- [40] Yun Liu, Krishna Gadepalli, Mohammad Norouzi, George E Dahl, Timo Kohlberger, Aleksey Boyko, Subhashini Venugopalan, Aleksei Timofeev, Philip Q Nelson, Greg S Corrado, et al. 2017. Detecting cancer metastases on gigapixel pathology images. arXiv preprint arXiv:1703.02442 (2017).
- [41] David N Louis, Hiroko Ohgaki, Otmar D Wiestler, Webster K Cavenee, Peter C Burger, Anne Jouvet, Bernd W Scheithauer, and Paul Kleihues. 2007. The 2007 WHO classification of tumours of the central nervous system. *Acta neuropathologica* 114, 2 (2007), 97–109.
- [42] Cheng Lu and Mrinal Mandal. 2013. Toward automatic mitotic cell detection and segmentation in multispectral histopathological images. *IEEE Journal of Biomedical and Health Informatics* 18, 2 (2013), 594–605.
- [43] William M Lydiatt, Snehal G Patel, Brian O'Sullivan, Margaret S Brandwein, John A Ridge, Jocelyn C Migliacci, Ashley M Loomis, and Jatin P Shah. 2017. Head and neck cancers—major changes in the American Joint Committee on cancer eighth edition cancer staging manual. *CA: a cancer journal for clinicians* 67, 2 (2017), 122–137.
- [44] Anne L Martel, Dan Hosseinzadeh, Caglar Senaras, Yu Zhou, Azadeh Yazdanpanah, Rushin Shojaii, Emily S Patterson, Anant Madabhushi, and Metin N Gurcan. 2017. An image analysis resource for cancer research: PIIP—pathology image informatics platform for visualization, analysis, and management. Cancer research 77, 21 (2017), e83–e86.
- [45] B Middleton, DF Sittig, and A Wright. 2016. Clinical decision support: a 25 year retrospective and a 25 year vision. *Yearbook of medical informatics* Suppl 1 (2016), S103.
- [46] Rashika Mishra, Ovidiu Daescu, Patrick Leavey, Dinesh Rakheja, and Anita Sengupta. 2018. Convolutional neural network for histopathological analysis of osteosarcoma. *Journal of Computational Biology* 25, 3 (2018), 313–325.
- [47] Lucio Palma, Paolo Celli, Carmine Franco, Luigi Cervoni, and Giampaolo Cantore. 1997. Long-term prognosis for atypical and malignant meningiomas: a study of 71 surgical cases. *Journal of neurosurgery* 86, 5 (1997), 793–800.
- [48] Liron Pantanowitz, Paul N Valenstein, Andrew J Evans, Keith J Kaplan, John D Pfeifer, David C Wilbur, Laura C Collins, and Terence J Colgan. 2011. Review of the current state of whole slide imaging in pathology. *Journal of pathology informatics* 2 (2011).
- [49] Emad A Rakha, Maysa E El-Sayed, Andrew HS Lee, Christopher W Elston, Matthew J Grainge, Zsolt Hodi, Roger W Blamey, and Ian O Ellis. 2008. Prognostic significance of Nottingham histologic grade in invasive breast carcinoma.

- Journal of clinical oncology 26, 19 (2008), 3153-3158.
- [50] Alexander Rakhlin, Alexey Shvets, Vladimir Iglovikov, and Alexandr A Kalinin. 2018. Deep convolutional neural networks for breast cancer histology image analysis. In *International Conference Image Analysis and Recognition*. Springer, 737–744.
- [51] Roy A Ruddle, Rhys G Thomas, Rebecca Randell, Philip Quirke, and Darren Treanor. 2016. The design and evaluation of interfaces for navigating gigapixel images in digital pathology. *ACM Transactions on Computer-Human Interaction (TOCHI)* 23, 1 (2016), 1–29.
- [52] Monjoy Saha, Chandan Chakraborty, Indu Arun, Rosina Ahmed, and Sanjoy Chatterjee. 2017. An advanced deep learning approach for Ki-67 stained hotspot detection and proliferation rate scoring for prognostic evaluation of breast cancer. *Scientific reports* 7, 1 (2017), 1–14.
- [53] Joel Saltz, Ashish Sharma, Ganesh Iyer, Erich Bremer, Feiqiao Wang, Alina Jasniewski, Tammy DiPrima, Jonas S Almeida, Yi Gao, Tianhao Zhao, et al. 2017. A containerized software system for generation, management, and exploration of features from whole slide tissue images. *Cancer research* 77, 21 (2017), e79–e82.
- [54] Caroline A Schneider, Wayne S Rasband, and Kevin W Eliceiri. 2012. NIH Image to ImageJ: 25 years of image analysis. *Nature methods* 9, 7 (2012), 671.
- [55] Ie-Ming Shih and Robert J Kurman. 1998. Ki-67 labeling index in the differential diagnosis of exaggerated placental site, placental site trophoblastic tumor, and choriocarcinoma: a double immunohistochemical staining technique using Ki-67 and Mel-CAM antibodies. *Human pathology* 29, 1 (1998), 27–33.
- [56] David F Steiner, Kunal Nagpal, Rory Sayres, Davis J Foote, Benjamin D Wedin, Adam Pearce, Carrie J Cai, Samantha R Winter, Matthew Symonds, Liron Yatziv, et al. 2020. Evaluation of the Use of Combined Artificial Intelligence and Pathologist Assessment to Review and Grade Prostate Biopsies. JAMA Network Open 3, 11 (2020), e2023267–e2023267.
- [57] Eliza Strickland. 2019. IBM Watson, heal thyself: How IBM overpromised and underdelivered on AI health care. IEEE Spectrum 56, 4 (2019), 24–31.
- [58] Peter Ström, Kimmo Kartasalo, Henrik Olsson, Leslie Solorzano, Brett Delahunt, Daniel M Berney, David G Bostwick, Andrew J Evans, David J Grignon, Peter A Humphrey, et al. 2020. Artificial intelligence for diagnosis and grading of prostate cancer in biopsies: a population-based, diagnostic study. The Lancet Oncology 21, 2 (2020), 222–232.
- [59] Mingxing Tan and Quoc Le. 2019. Efficientnet: Rethinking model scaling for convolutional neural networks. In International Conference on Machine Learning. PMLR, 6105–6114.
- [60] Randy L Teach and Edward H Shortliffe. 1981. An analysis of physician attitudes regarding computer-based clinical consultation systems. Computers and Biomedical Research 14, 6 (1981), 542–558.
- [61] Philipp Tschandl, Christoph Rinner, Zoe Apalla, Giuseppe Argenziano, Noel Codella, Allan Halpern, Monika Janda, Aimilios Lallas, Caterina Longo, Josep Malvehy, et al. 2020. Human–computer collaboration for skin cancer recognition. Nature Medicine 26, 8 (2020), 1229–1234.
- [62] Brian Patrick Walcott, Brian V Nahed, Priscilla K Brastianos, and Jay S Loeffler. 2013. Radiation treatment for WHO grade II and III meningiomas. Frontiers in oncology 3 (2013), 227.
- [63] Dayong Wang, Aditya Khosla, Rishab Gargeya, Humayun Irshad, and Andrew H Beck. 2016. Deep learning for identifying metastatic breast cancer. arXiv preprint arXiv:1606.05718 (2016).
- [64] Shidan Wang, Donghan M Yang, Ruichen Rong, Xiaowei Zhan, Junya Fujimoto, Hongyu Liu, John Minna, Ignacio Ivan Wistuba, Yang Xie, and Guanghua Xiao. 2019. Artificial intelligence in lung cancer pathology image analysis. *Cancers* 11, 11 (2019), 1673.
- [65] Nora S Willett, Rubaiat Habib Kazi, Michael Chen, George Fitzmaurice, Adam Finkelstein, and Tovi Grossman. 2018.
 A mixed-initiative interface for animating static pictures. In Proceedings of the 31st Annual ACM Symposium on User Interface Software and Technology. 649–661.
- [66] Yao Xie, Melody Chen, David Kao, Ge Gao, and Xiang'Anthony' Chen. 2020. CheXplain: Enabling Physicians to Explore and Understand Data-Driven, AI-Enabled Medical Imaging Analysis. In *Proceedings of the 2020 CHI Conference on Human Factors in Computing Systems.* 1–13.
- [67] Fuyong Xing, Toby C Cornish, Tell Bennett, Debashis Ghosh, and Lin Yang. 2019. Pixel-to-pixel learning with weak supervision for single-stage nucleus recognition in Ki67 images. IEEE Transactions on Biomedical Engineering 66, 11 (2019), 3088–3097.
- [68] Qian Yang, Aaron Steinfeld, Carolyn Rosé, and John Zimmerman. 2020. Re-examining Whether, Why, and How Human-AI Interaction Is Uniquely Difficult to Design. In Proceedings of the 2020 chi conference on human factors in computing systems. 1–13.
- [69] Qian Yang, John Zimmerman, Aaron Steinfeld, Lisa Carey, and James F Antaki. 2016. Investigating the heart pump implant decision process: opportunities for decision support tools to help. In Proceedings of the 2016 CHI Conference on Human Factors in Computing Systems. 4477–4488.
- [70] Choon K Yap, Emarene M Kalaw, Malay Singh, Kian T Chong, Danilo M Giron, Chao-Hui Huang, Li Cheng, Yan N Law, and Hwee Kuan Lee. 2015. Automated image based prominent nucleoli detection. *Journal of pathology informatics* 6

xPath: Human-Al Diagnosis in Pathology with Multi-Criteria Analyses and Explanation by Hierarchically Traceable Evidence

31

(2015).

[71] Zongwei Zhou, Md Mahfuzur Rahman Siddiquee, Nima Tajbakhsh, and Jianming Liang. 2018. Unet++: A nested u-net architecture for medical image segmentation. In *Deep Learning in Medical Image Analysis and Multimodal Learning for Clinical Decision Support*. Springer, 3–11.